Synthetic modification of fusogenic coiled coil peptides

Crone, N.S.A.

5.

Azobenzene-based amino acids for photocontrol of coiled coil peptides

This chapter is in preparation as an original research paper: Niek S.A. Crone, Niek v. Hilten, Alex v.d. Ham, Aimee L. Boyle, Alexander Kros, **2021**.

Abstract

Coiled coil peptides have been under investigation as binding motifs in synthetic biology and biomaterials, with active control over their self-assembly allowing for a wider range of applications. To introduce photocontrol in coiled-coil assembly, three azobenzene-containing amino acids were prepared and incorporated into the hydrophobic core of the heterodimeric coiled coil formed between peptide 'K_3', $(KIAALKE)_3$ and peptide 'E_3' $(EIAALEK)_3$. Two amino acids (**APhe1** and **APhe2**) were based on phenylalanine, differing in the presence of a carboxylic acid group, and have previously shown to allow photomodulation of protein activity. When incorporated in peptide K_3, binding to peptide E_3GY changed upon *trans* to *cis* isomerization, with the two variants differing in the most folded state. The third azobenzene-containing amino acid, **APgly**, is a novel design based on phenylglycine, and showed comparable absorption bands and isomerization to the phenylalanine based amino acids. When **APgly** was incorporated in the coiled-coil, a 4.7-fold decrease in folding constant was observed upon *trans* to *cis* isomerization, the largest difference for all three amino acids. Removal of the methylene group was theorized to position the diazene closer to the hydrophobic amino acids and reduce the possible rotations of the amino acid, with molecular dynamics simulations supporting these hypotheses. Combined, these results show **APgly** as a novel photoswitchable amino acid for the photocontrol of coiled-coil assembly. The introduction of **APgly** in existing coiled-coil based biomaterials should therefore allow for control over activity related to coiled-coil formation.

5.1 Introduction

In **Chapter 4**, the photocontrol of coiled-coil peptide assembly was investigated via intramolecular cyclization using an azobenzene-based crosslinker. This cyclization-based strategy affects peptide structure by providing an energetic constraint on the length of the crosslinked region, and by design does not interact with the amino acid side chains taking part in coiled-coil formation.[1] Because the crosslinking strategy proved to be a major bottleneck in the preparation of photoactive peptides, alternative methods were sought. Therefore, in this chapter, the incorporation of azobenzene-based amino acids into the hydrophobic positions of coiled-coil peptides is investigated as a novel method for coiled-coil photocontrol.

Single amino acid modifications in the hydrophobic domain of coiled-coil forming peptides have been investigated both to aid understanding of coiled-coil assembly, and to introduce selectivity or functionality. For example, the group of Hodges investigated substitution at the 'a' position of a cysteine-crosslinked homotrimeric system,[2] and, in a separate study, the role of the 'd' position in a crosslinked homodimeric peptide.[3] The two positions showed a different preference for amino acids, with the general trend being that hydrophobic amino acids stabilize, and polar or charged amino acids destabilize, coiled-coil formation relative to alanine. When comparing aromatic amino acids, phenylalanine and tyrosine are well tolerated but the large double ring system of tryptophan does not provide higher stability compared to alanine. Acharya *et al.* performed single amino acid substitutions in the basic leucine zipper protein VBP, and observed changes in the Gibbs free energy of binding of up to 9.2 kcal/mol by substituting opposing amino acids in the 'a' position.[4, 5] Although not all possible amino acids were investigated, the same trend was observed as previously shown by the group of Hodges, and the effect remained when both chains were substituted. The role of asparagine in the hydrophobic core has also been investigated, because it is a common feature in natural coiled-coil peptides, and is useful to control peptide oligomerization although at a cost of overall stability of the coiled coil.[6, 7] To introduce a response to an external trigger, redox switching of methionine residues in the hydrophobic core has been investigated and results in disruption of the coiled coil,[8] and substitution of hydrophobic amino acids for histidine residues leads to self-assembly which is dependent on pH or metal ion coordination in a trimeric coiled-coil system.[9-11] This previous work on hydrophobic core modifications suggests that

the incorporation of azobenzene-based amino acids, which change structure and polarity via *cis*/*trans* isomerization through light illumination (see **Chapter 4**), should allow for control over coiled-coil assembly.

Phenylazo-phenylalanine (**APhe1**, **Scheme 5.1**) was one of the first published amino acids containing an azobenzene moiety,[12] and has been incorporated into synthetic peptides and into protein structures via genetic code expansion.[13] To date, **APhe1** and structural derivatives have been used to control enzyme dimerization necessary for catalytic activity,[14, 15] the DNA binding strength of the CAP transcription factor by destabilization of its cAMP binding site,[13] incorporation into superfolder green fluorescent protein,[16] and allosterically reducing the protein-ligand binding strength in chemiluminescent luciferase or subunit interaction in imidazole glycerol phosphate synthase.[17, 18] Derivatives of **APhe1** containing reactive sites for the generation of intramolecular crosslinked proteins have also been studied for control over helical folding,[19, 20] similar to the crosslinking strategy investigated in the previous chapter. Since its incorporation into peptides and proteins has been demonstrated to be straightforward, the potential ability of **Aphe1** derivatives to control coiled-coil assembly would provide a novel method for the introduction of photoswitching into a wide variety of natural and synthetic coiled-coil systems already under investigation.[21, 22]

To test whether azobenzene-based amino acids can be used to control coiled-coil folding, peptides incorporating three structurally diverse non-natural amino acids were prepared by solid phase peptides synthesis (SPPS). Two of the amino acids were derived from L-phenylalanine, namely **Aphe1** and **Aphe2**, and these differ in

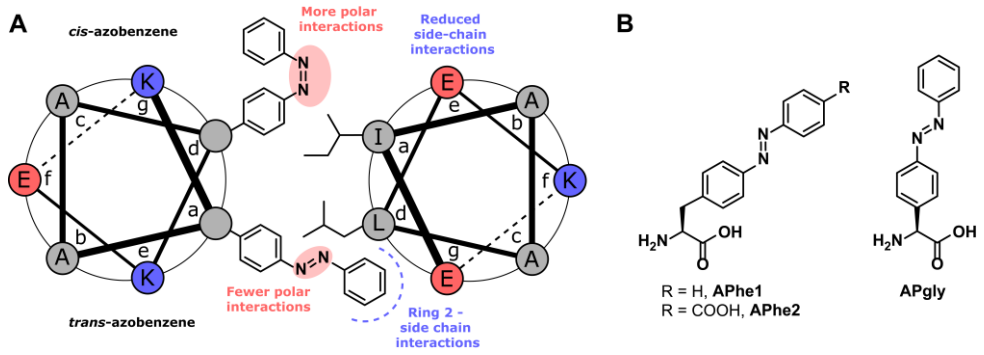

Scheme 5.1: Hypothesized interactions of azobenzene in the coiled-coil hydrophobic core (A), and the three azobenzene based amino acids investigated in this chapter for the control over coiled-coil self-assembly (B).

the presence of a carboxylic acid group *para* to the diazene group for **APhe2** (**Scheme 5.1B**). The carboxylic acid present in **APhe2** is theorized to introduce electrostatic repulsion with the opposing glutamic acid residue, destabilizing the coiled coil when the azobenzene is in the *trans* conformation. Switching electrostatic interactions has been investigated previously via enzymatic serine phosphorylation,[23] and allowed both stronger and weaker interactions after phosphorylation depending on the design.[24] Besides azobenzene derivatives of L-phenylalanine, the azobenzene derivative of L-phenylglycine was prepared (**APgly**, **Scheme 5.1B**), with the expectation that this amino acid would result in a better incorporation in the hydrophobic core compared to **APhe1** due to the absence of a methylene group. The three azobenzene-based amino acids were incorporated into a dimeric coiled-coil which is used in our group as a SNARE protein mimic.[25] This coiled-coil system consists of peptide 'K_3', $(KIAALKE)_3$ and peptide 'E_3' $(EIAALEK)_3$, which self-assemble into a dimeric parallel coiled-coil with high binding affinity.[26] After incorporation in peptide K_3, **APgly** showed the largest difference in coiled-coil binding upon *trans* to *cis* isomerization, with a 4.65 fold decrease in the folding constant. Molecular dynamics (MD) simulations of **APhe1** and **APgly** in the coiled coil show more rearrangement of the **APhe1** azobenzene after isomerization, and support **APgly** as a better switch for coiled-coil photocontrol.

5.2 Results and Discussion

Peptides containing azobenzene derivatives of phenylalanine.

Photoswitchable amino acids based on phenylalanine were prepared following literature procedures (**Scheme 5.2**),[14] with the 9-fluorenylmethoxy-carbonyl (Fmoc) protecting group on the α-amine to facilitate use in SPPS. Fmoc-4-nitro-l-phenylalanine, **1**, was prepared from L-phenylalanine via nitration and Fmoc-protection, or was purchased commercially. Subsequently the nitro group of **1** was reduced to the respective aniline with Zn powder and ammonium chloride, followed by a Mills reaction with nitrosobenzene to yield N^{α}-fmoc-4-(phenylazo)-L-phenylalanine, **2**. The same procedure was followed for the preparation of protected **APhe2**, utilizing *tert*-butyl-4-nitrosobenzoate in the Mills reaction resulting in product **3**. The tert-butyl ester is used to prevent side reactions during SPPS, and is removed by the acidic peptide cleavage conditions to yield the carboxylic acid. Derivatives of peptide K_3 (sequence shown in **Scheme 5.2**) were prepared via SPPS, with the isoleucine at position 9 replaced with **APhe1** or **APhe2.**

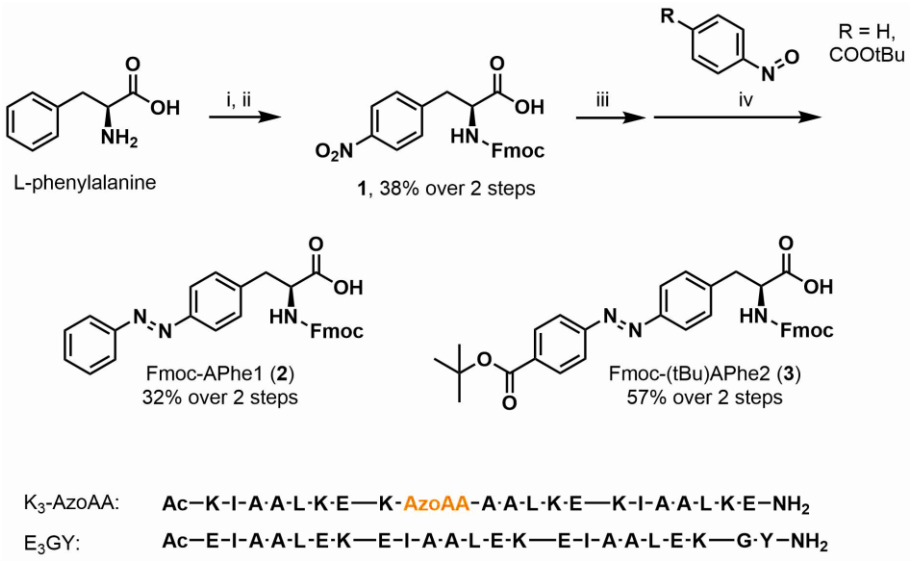

Scheme 5.2: Reaction scheme for the preparation of azobenzene containing amino acids based on phenylalanine (top) and amino acid sequences of peptides prepared in this chapter (bottom). AzoAA refers to APhe1, APhe2 or APgly. Reagents and conditions: (i) HNO_3, H_2SO_4; (ii) Fmoc-chloride, $NaHCO_3$; (iii) Zn powder, NH_4Cl, EtOH; (iv) AcOH.

The UV absorption spectra of the two peptides were very similar (**Figure 5.1A**),with a slight redshift for the absorption bands of **APhe2** (335 nm, ε = 9,480 M^{-1} cm^{-1}) compared to **APhe1** (327 nm, ε = 10,020 M^{-1} cm^{-1}). Both amino acids could be isomerized to the *cis* conformation with 340 nm light, as observed by the disappearance over time of the strong absorption peak (**Figure S5.1**). *Cis* to *trans* isomerization from the 340 nm photostationary state (PSS) could be achieved efficiently with 435 nm light (**Figure 5.1B**). After plotting the change in intensity of the absorption maximum in the dark-adapted state, a larger difference after 340 nm irradiation is observed for **APhe1**, indicating this amino acid is isomerized to the *cis* conformation more completely by 340 nm light, or the *cis* conformer of **APhe2** has a stronger absorption band (**Figure 5.1C**). Back isomerization from *cis* to *trans* with 435 nm light is slightly more efficient for **APhe2**, resulting in 98% of the absorption maximum observed in the dark state, compared to 92% for **APhe1**.

The structure of the K_3 peptides and coiled coils was studied via CD spectroscopy to determine the effect of phenylalanine-based photoswitches on peptide folding. Peptide E_3GY was used as binding partner, since the tyrosine can be used to accurately determine peptide concentration. Both **K_3-APhe1** and **K_3-APhe2** peptides were mostly unstructured by themselves, and able to form coiled coils in

combination with E_3GY (**Figure 5.2**), with only marginal differences in structure between the dark adapted and 340 nm irradiated states. Because no obvious differences in structure were observed after irradiation, thermal denaturation experiments were performed to determine whether the binding affinity was dependent on sample irradiation. For this, CD melting curves measured at different concentrations were fitted to a coiled-coil binding model (**Figure S5.2** and **Figure S5.3**).[27] The best fit was achieved for a dimeric coiled coil over other oligomeric states, and important parameters from this fitting are shown in **Table 5.1**.

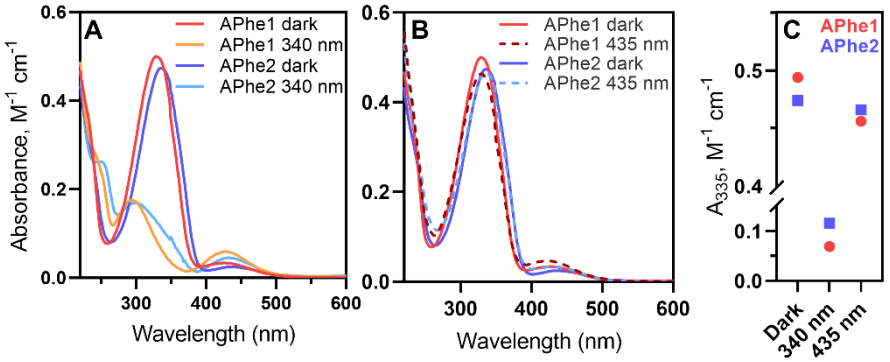

Figure 5.1: UV spectra of peptide K_3 with position 9 changed for **APhe1** or **APhe2**, showing spectra for the dark-adapted peptide and after *trans* to *cis* isomerization with 340 nm light (A). Spectra after *cis* to *trans* isomerization using 435 nm light (B), and an overview of the absorbance at 335 nm for the dark adapted, 340 nm PSS and 435 nm PSS (C). [Peptide] = 50 µM in PBS buffer.

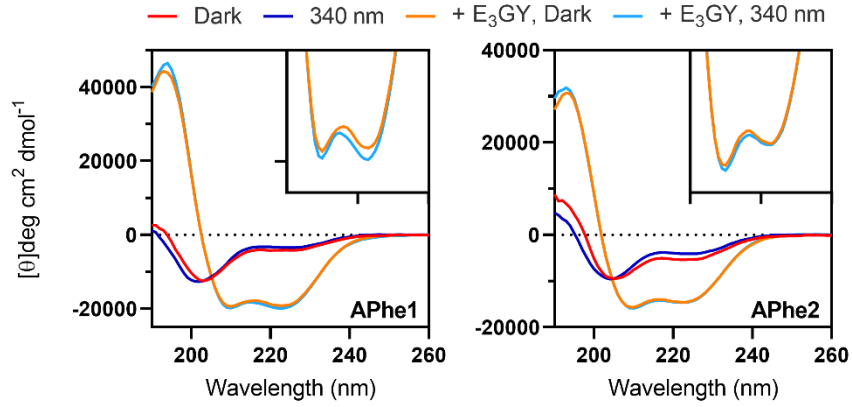

Figure 5.2: CD spectra of peptide K_3 with the 9th amino acid changed for **APhe1** or **APhe2**, showing both the dark adapted and 340 nm irradiated states, as well as spectra with and without binding partner E_3GY. All samples were measured in 10 mM phosphate containing 2 mM NaCl, with [peptide] = 50 µM.

Table 5.1: Fit results of CD thermal unfolding curves from **APhe1-**, or **APhe2**-containing K_3 as a coiled-coil with E_3GY. A complete list of fitting parameters and confidence intervals can be found in **Table S5.1**.

Parameter	K_3-APhe1 Dark	K_3-APhe1 340nm	K_3-APhe2 dark	K_3-APhe2 340nm
$\Delta H°$[a] (kJ mol^{-1})	224.7	261.4	175.0	259.0
T°[a] (°C)	123	114.1	142.5	102.1
ΔC_p[b] (kJ mol^{-1} k^{-1})	1.69	2.46	1.07	2.65
K_f (M^{-1})[c]	9.19 10^5	7.09 10^5	2.18 10^5	3.26 10^5
K_u (µM)[c]	**1.09**	**1.41**	**4.58**	**3.07**
Dark/340nm PSS		1.30		0.67

[a] $\Delta H°$ and T° are the enthalpy and the temperature where $\Delta G = 0$ and $K_U = K_F = 1$. [b] ΔC_P is the change in heat capacity upon unfolding. [c] Binding model at 20 (°C).

Photoisomerization of **K_3-APhe1** using 340 nm light resulted in an increase in the unfolding constant K_u, from 1.09 to 1.41 µM, showing reduced coiled-coil binding in the irradiated state. The opposite was observed for **K_3-APhe2**, where irradiation yielded a reduction in K_u from 4.58 to 3.07 µM, revealing the 340 nm irradiated state to contain the most stable coiled-coil. The carboxylic acid group in **APhe2** is intended to increase electrostatic repulsion with glutamic acid residues of E_3 in the *trans* conformation, resulting in the *cis* conformation as the most stable coiled-coil. Contrary to our expectations, the *cis* isomer of **K_3-APhe1** was not the most stable state, showing that the bulk of the *trans* azobenzene moiety is better accommodated in the hydrophobic positions of the coiled-coil, than the increased polarity of the diazene in the *cis* conformation. In summary, incorporation of **APhe1** and **APhe2** in the coiled-coil hydrophobic core was successful, but the design of these amino acids needs to be improved since the difference in coiled-coil formation between the dark state and 340 nm PSS was small.

Given the small differences observed for the peptides modified with azo derivatives of phenylalanine, a different amino acid structure was designed. Removal of the methylene group from **APhe1** results in a phenylglycine derivative that was theorized to position the diazene closer to the side chain of hydrophobic amino acids in the 'a' and 'd' positions, and increase the effect of photoisomerization. Amino acid 4-(azophenyl)phenylglycine (**APgly**, **Scheme 5.1**) was chosen to test this theory due to its structural simplicity.

Synthesis and peptide incorporation of 4-(Azophenyl)phenylglycine

Synthesis of N-fmoc-4-(phenylazo)-L-phenylglycine (Fmoc-APgly, **10**, **Scheme 5.3**) follows the same general route as the synthesis of azobenzene derivatives of phenylalanine; preparation of the *para*-substituted aniline followed by a Mills reaction with nitrosobenzene to yield the azobenzene. Preparation of the aniline requires an alternative method, since nitration of phenylglycine does not yield the *para*-nitrated product, and preparation of the 4-nitro variant via a Strecker

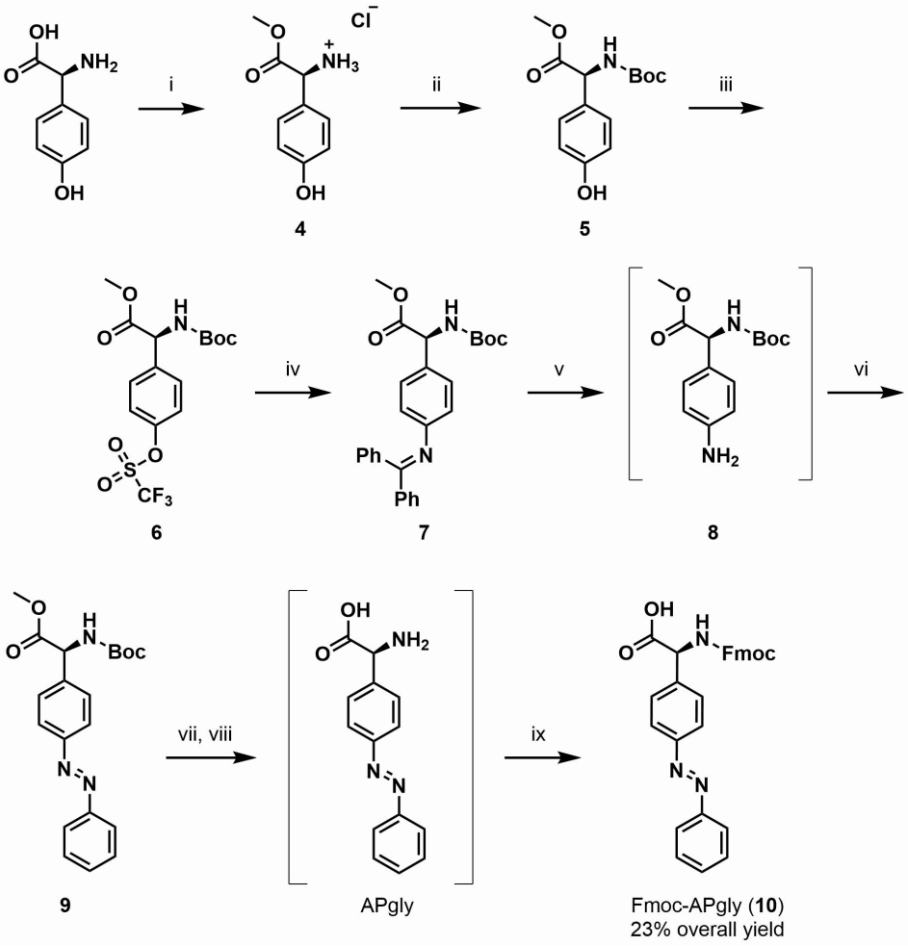

Scheme 5.3: Synthetic scheme for the preparation of Fmoc-APgly from 4-hydroxyphenylglycine. Reagents and conditions: (i) MeOH, $SOCl_2$, 0 °C to RT, 95%; (ii) Boc_2O, TEA, MeCN, 93%; (iii) Tf_2O, TEA, DCM, -20 °C to RT, 98% (88% from **5**); (iv) Benzophenone imine, *rac*-BINAP, $Pd(OAc)_2$, Cs_2CO_3, PhMe, 100 °C, 65%; (v) NH_4HCO_2, 10% Pd/C, MeOH, 60 °C; (iv) Nitrosobenzene, AcOH, 74% over 2 steps; (vii) LiOH, H_2O/THF; (viii) TFA, DCM; (ix) Fmoc-chloride, $NaHCO_3$, H_2O/THF, 63% over 3 steps.

synthesis is not effective.[28] Therefore, amination of the respective aryl triflate (**6**) was deemed the most effective route, since the 4-hydroxy precursor is readily available. This route was tried and ultimately effective in the amination of **6** in sufficient quantities, from which **10** could be prepared following the procedure described below.

Methylation of 4-hydroxy-L-phenylglycine to form ester **4** was followed by amine protection with Boc anhydride to yield the double protected amino acid **5**, followed by installation of the aryl triflate to form intermediate **6** in high yields. Initially the use of zinc trimethylsilylamide as an ammonia equivalent was attempted in the palladium-catalysed amination of **6**,[29] but the use of benzophenone imine proved much more effective, producing intermediate **7** in 65% yield.[30] The imine was then reduced to yield aniline **8**, followed directly by the Mills reaction to form azobenzene **9**. Ester hydrolysis and Boc deprotection yielded **APgly**, which was Fmoc-protected to yield product **10**. The final three steps could be performed in good (63%) overall yield, however attempts to simplify the procedure in the form of a one-pot procedure resulted in a sharp reduction in product yield. The overall yield of **10** from 4-hydroxy-L-phenylglycine is good (23% over 9 steps), yet the atom efficiency could be improved as most steps concern protecting group manipulation. Since only mildly basic conditions are used for the conversion of **5** to **9**, for the larger scale synthesis of **10** the amination of Fmoc-protected phenylglycine- 4-triflate would be worth investigating, as it would eliminate 4 synthetic steps.

As azobenzene photoswitches based on phenylglycine have not been reported, the photoswitching behaviour of Fmoc-APgly (**10**) was analysed, as displayed in **Figure 5.3**. High-pressure liquid chromatography (HPLC) separation of **10** dissolved in MeCN and kept under dark conditions, showed predominantly the *trans* (94.2 ± 0.2%) isomer, which switches to predominantly *cis* (91.3 ± 0.6%) when irradiated with 340 nm light (**Figure 5.3C**). The largest proportion of *trans* to *cis* isomers achieved via photoisomerization was after irradiation with 385 nm light (83.2 ± 0.2% *trans*), although higher wavelengths showed very similar distributions. No difference was observed in the proportions of isomers when **10** was directly illuminated with 435 nm light, or first isomerized to be *cis*-dominant with 340 nm light followed by illumination with 435 nm light, as is expected for the PSS. Relaxation after irradiation with 340 nm light was tracked over time (**Figure 5.3B**), and showed proportional decline of the *cis* isomer and increase in *trans* isomer,

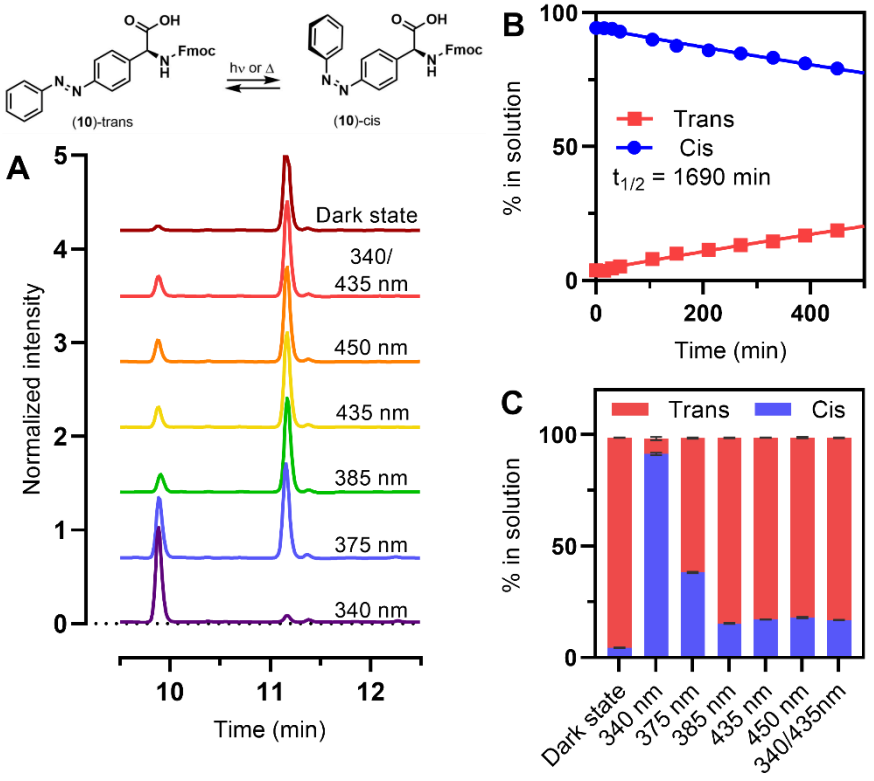

Figure 5.3: HPLC traces of Fmoc-APgly, showing the chromatogram of the compound after irradiation with different wavelengths of light (A), thermal relaxation back from *cis* to *trans* (B), and the percentage of the *trans* and *cis* isomers in solution at the different photostationary states (C). All illuminations and relaxation studies were performed in MeCN at 20 °C.

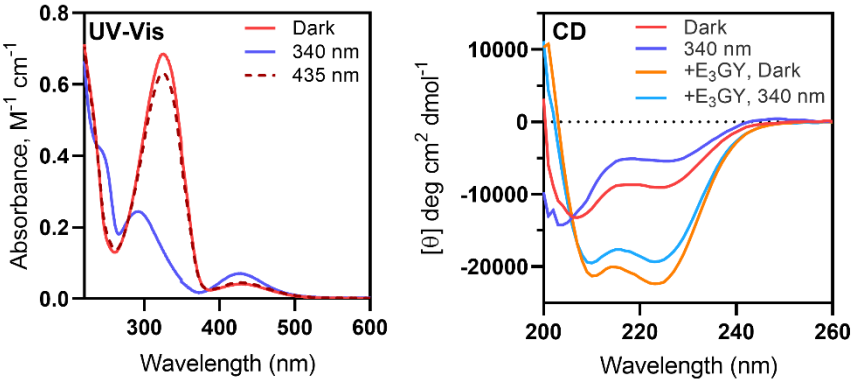

Figure 5.4: UV-Vis (left) and CD (right) spectra of peptide K_3-APGly during photoswitching. Spectra are recorded with samples that were dark adapted, or irradiated with light until no changes could be observed. Spectra were recorded at 20 °C in PBS with [peptide] = 50 µM.

Table 5.2: Fit results of CD thermal unfolding curves from **K_3-APgly** as a coiled-coil with E_3GY. A complete list of fitting parameters and confidence intervals can be found in **Table S5.2**.

Coiled-coil system	**K_3-APgly dark**	**K_3-APgly 340nm**
$\Delta H°^a$ (kJ mol^{-1})	285.2	236
$T°^b$ (°C)	113.0	110.5
ΔC_p (kJ mol^{-1} k^{-1})	2.80	2.15
K_f (M^{-1})^c	1.38 x 10^6	2.97 x 10^5
K_u (μM)^c	**0.72**	**3.37**
Dark/340nm PSS		4.65

[a] $\Delta H°$ and T° are the enthalpy and the temperature where $\Delta G = 0$ and $K_U = K_F = 1$. [b] ΔC_P is the change in heat capacity upon unfolding. [c] Binding model at 20 (°C).

with a half-life of 1690 minutes (≈ 28 h), comparable to reported half-lives for **APhe1** (1600 min) and **APhe2** (2100 min).[14]Incorporation of **10** in K_3 was achieved using normal Fmoc-SPPS methods. UV-Vis Spectra of **K_3-APgly** in PBS showed a strong absorbance band at 325 nm (**Figure 5.4**, ε = 13,700 M^{-1} cm^{-1}) that disappeared upon irradiation with 340 nm light, demonstrating *trans* to *cis* isomerization, accompanied by an increase in the absorbance at 428 nm. Irradiation of the sample with 435 nm light resulted in 92% of the dark absorbance at 325 nm, showing effective *cis* to *trans* isomerization. The observed absorbance values in UV-Vis are in agreement with the isomeric ratios observed with HPLC (**Figure 5.3A**), demonstrating that **APgly** incorporation in peptides does not affect isomerization. CD spectra of **K_3-APgly** showed a partially folded helix in the dark, that becomes less structured when irradiated with 340 nm light. Addition of binding partner E_3GY led to a well-folded coiled-coil, that also showed a reduction in signal upon isomerization. The difference in folding between dark adapted and irradiated samples is much larger for peptide K_3 containing **APgly**, than it was for either of the phenylalanine derivatives, showing that the azobenzene is better positioned for coiled-coil photocontrol in the **APgly** derivative. The effect of isomerization on coiled-coil binding strength was again determined using thermal denaturation titration experiments (**Figure S5.4**), with fitting parameters shown in **Table 5.2** and **Table S5.2**. The coiled-coil formed by **K_3-APgly** and E_3GYwas determined to have a K_u of 0.72 μM in the dark, which increased to 3.37 μM after photoisomerization. This equates to a 4.65-fold reduction in binding affinity for **K_3-APgly** by isomerization of the azobenzene to the *cis* dominant state.

The difference between the dark and 340 nm adapted state is larger for **K_3-APgly** then was observed for either of the peptides that incorporated the phenylalanine derivatives, and the overall highest folding constant was also observed for this peptide. When comparing **APgly** isomerization to amino acid substitution at position 'a' studied by the group of Hodges,[2] the change in binding energy is similar to substitution of alanine by a polar (Ser) or basic (Lys) side chain.

For the potential application of **K_3-APgly** in an active (fusion) system, stability of the photoswitch to repeated light exposures (photocycling) is an important characteristic. A solution of **K_3-APgly** was illuminated repeatedly first with 340 nm, followed by 435 nm light, and the switching monitored via the UV absorbance band at 325 nm (**Figure 5.5** and **Figure S5.5**). The azobenzene consistently yielded the same absorption maxima during 6 cycles, demonstrating cycling of photostationary states with minimal deviation. Finally, the peptide was irradiated to the 340 nm PSS and allowed to thermally relax, showing 65% recovery in 69 hours. This thermal relaxation is 1.6 times slower ($t_{1/2}$ = 46h) than observed for **10** in MeCN, which can be explained by the increased dielectric constant of the solvent.[31]

Molecular simulations

In the previous experiments we have shown that incorporation of an azobenzene amino acid in the hydrophobic core of the K_3/E_3 coiled-coil yields more effective

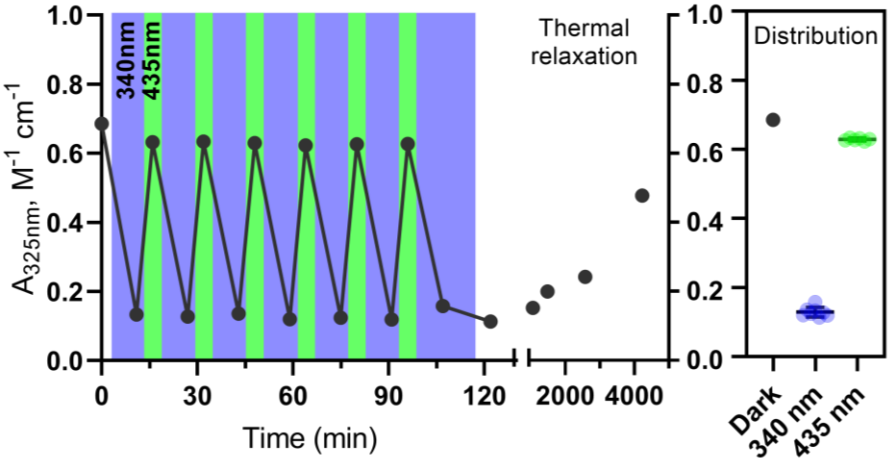

Figure 5.5: Photocycling of K_3-APgly between the dark adapted, 340 nm and 435 nm PSS (left), thermal relaxation of the peptide after thermal cycling (middle) and distribution of the absorbance in the different states during cycling (right). Absorbance at 325nm is plotted (full spectra are displayed in **Figure S5.5**), measurements were performed at 20 °C in PBS with [Peptide] = 50 µM.

photoswitching when it is derived from phenylglycine then from phenylalanine. To understand how one methylene group affects azobenzene interactions, molecular models of **K_3-APgly** and **K_3-APhe1** were prepared. These models were based on the NMR structure of the K_3/E_3 coiled-coil,[32] but with the Ile residue at position 9 replaced by a geometry optimized model of the synthetic amino acids in the *cis* or *trans* conformations. 500 ns MD simulations of these initial helical models were performed, with all 4 peptides showing a mostly stable helical coiled-coil structure during the simulations (**Figure S5.6**), although some unfolding at the termini was observed.

Snapshots from these MD simulations, displaying the azobenzene-amino acid and all side chains of peptide E_3 within 5 Å of that residue are shown in **Figure 5.6**. For both peptides, the azobenzene is shown to be close to the hydrophobic amino acids (Leu5, Ile9, Leu12) in the 'a' and 'd' positions, as well as adjacent amino acids (Ala4, Glu8) in the 'g' and 'c' positions. Both azobenzene amino acids extend outside of hydrophobic core, therefore shielding of the azobenzene outer phenyl group (as viewed from the backbone, and referred to as 'Ring 2') from the surrounding water by amino-acid side chains will have an impact on coiled-coil stability. The snapshot of *cis* **K_3-APgly** places the diazo group in the same position as in the *trans* conformation, with ring 2 rotated towards peptide K. The opposite is observed in the snapshots of **K_3-APhe1**, where the diazene group is in a different position relative to K_3 and ring 2 is still able to interact with amino acids in peptide E_3.

Because snapshots are not representative of the entire simulations, the average change in distance between the azobenzene and the amino acids of E_3 over all simulations was determined (**Figure 5.7** and **Figure S5.8**). Distance changes to the diazene, ring 1 and ring 2 were plotted separately, since different interactions are expected for these groups. Both the diazene and ring 2 of **APhe1** show a negative distance change for amino acids close to the C-terminus, indicating closer positioning to those groups in the *cis* conformation, which changes to positive values when moving through the sequence. A normalized change in distance ≤ -0.2 or ≥ 0.2 was deemed 'significant' in order to compare the different groups and photoswitches. More significant distance changes are observed for ring 2, which is expected since it is further away from the isomerized diazene, and therefore any rotation is amplified. All amino acids in the 'a', 'c', 'd' and 'g' positions of E_3 show significant changes in distance to **APhe1**, with the other three positions also showing some significant changes. The apparent crossover point observed in the

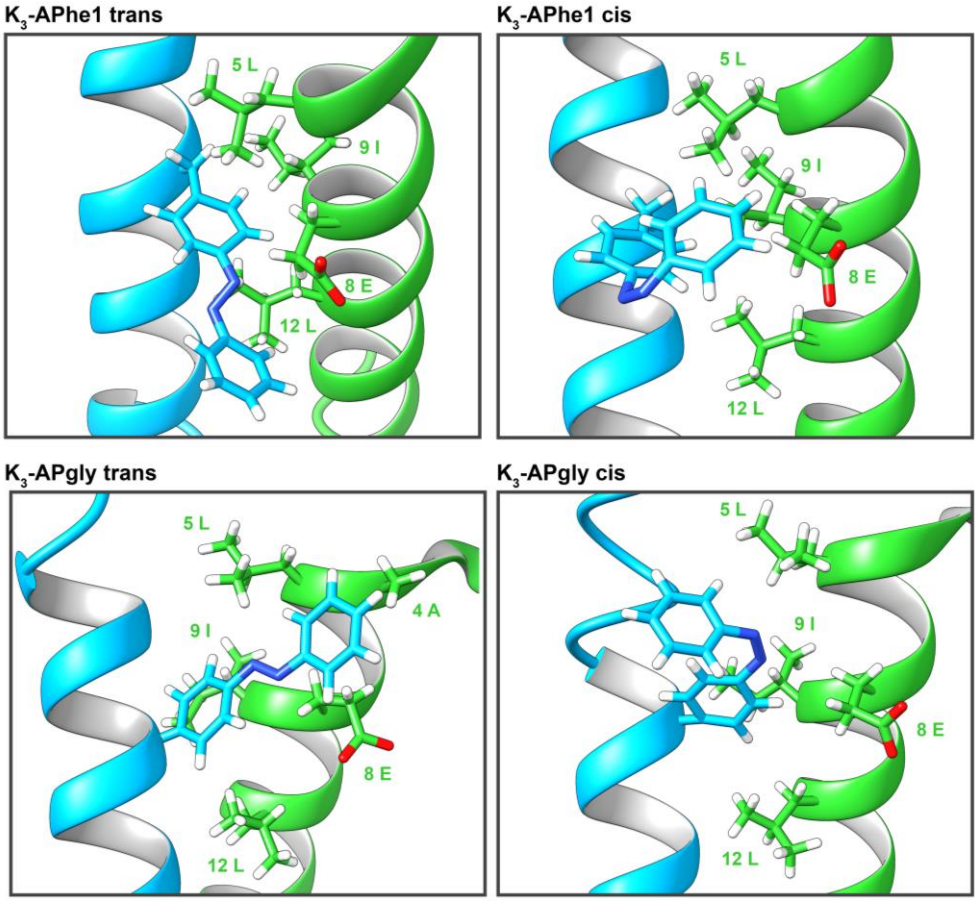

Figure 5.6: Snapshot from MD simulations of the coiled coil between peptide K_3 (blue) and E_3 (green), with peptide K_3 containing the photoswitchable amino acid **APhe1** or **APgly** in the *trans* or *cis* conformation. Peptides backbones are shown as a cartoon, with the photoswitch and all amino acid side chains of peptide E_3 within 5 Å displayed as sticks. Representative snapshots were chosen based on a similar RMSD from an ideal helix. Complete images are shown in **Figure S5.7**.

distance change graphs, combined with significant changes in distance upon **APhe1** isomerization for nearly all amino acids suggests reorganization after isomerization, where the azobenzene can move to a different conformation to accommodate the *cis* isomer. This is supported by the distance change for ring 1 (**Figure S5.8**), which shows the same general distribution of distance change throughout the sequence.

Peptide **K_3-APgly** shows the largest change in distance for Leu side chains in the 'd' position of the heptad repeat sequence of E_3, and to the Glu side chain at position8. There are more distinct changes in distance to side chains in the 'a' and 'c' positions,

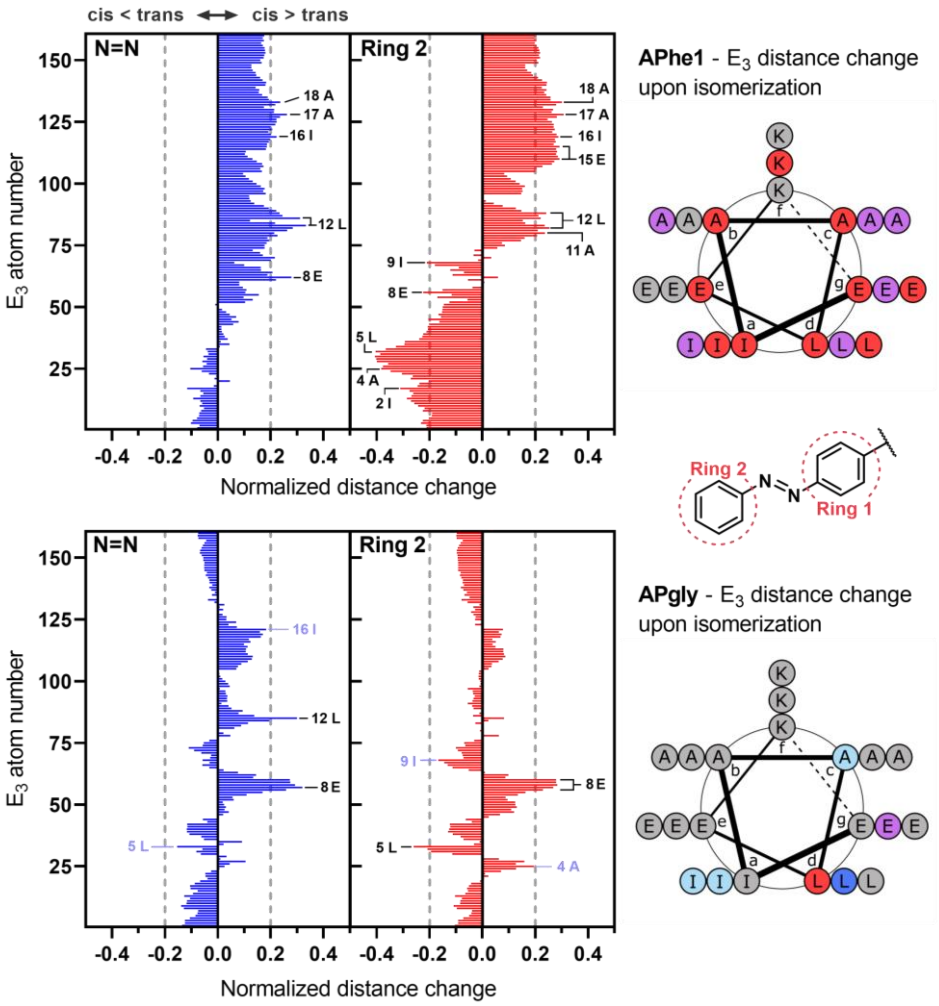

Figure 5.7: Normalized change in distance upon photoisomerization between the non-hydrogen atoms in peptide E_3 and the azobenzene diazene or ring 2 (left) during MD simulations, and helical wheel diagrams of peptide E_3 indicating the positions of the amino acids with significant changes in distance (right). Change in distance upon *trans* to *cis* isomerization of the azobenzene is normalized to the *trans* simulations, with positive values indicating more distance in the *cis* simulations. Distances are averaged over 3 simulations of 500 ns. Dotted lines indicate an arbitrary cut-off for significance of 0.2, with amino acids of interest marked light blue if their value falls below this line. Amino acids in the helical wheel diagram are coloured to indicate significant differences to the diazo group (blue), ring 2 (red), or both (purple), with amino acids of interest which fall below the cut-off also coloured light blue.

but these fall outside of the significance threshold that we use for comparison and have been marked with a lighter colour in **Figure 5.7**. Isomerization to *cis* is expected to result in repulsion of the diazene by hydrophobic side chains, which is

observed in the increased distance for Leu12 and Glu8, which are directly opposite the azobenzene in the coiled coil. After isomerization, ring 2 of **APgly** shows positioning close to amino acid side chains of K_3 (**Figure S5.9**), which stabilizes the *cis* conformation. Overall, the photoswitch of **K_3-APgly** shows changes in distance with the amino acids that are already closely positioned in the *trans* conformation, indicating the changes in distance can be attributed to the rotation around the diazene bond after isomerization.

If we generalize the structures in the MD snapshots with the changes in distance shown in **Figure 5.7**, the effect of isomerization on the coiled-coil folding constant observed in the previous section can be explained. Upon *trans* to *cis* isomerization, the diazene group becomes more polar resulting in unfavourable interactions if it is positioned in the hydrophobic core, and with both azobenzene amino acids, a general increase in distance to the diazene is observed. **APhe1** has two bonds between C_α and the azobenzene moiety, which allows for more degrees of freedom to reposition the azobenzene after isomerization compared to **APgly**, which can only change position via a single rotation and deviation from the optimal bond angles. The extra rotational freedom in **APhe1** results in a decreased effect of the diazene polarity on coiled-coil stability through repositioning of the azobenzene. This repositioning also allows ring 2 to keep interacting with (different) hydrophobic side chains from peptide E_3, which is not possible for **K_3-APgly**. Both of these factors decrease the differences in binding strength between the two isomeric states of **APhe1**, and explain why **APgly** shows the largest difference in coiled-coil binding upon isomerization.

5.3 Conclusions

Two azobenzene derivatives of phenylalanine, **APhe1** and **APhe2**, were prepared and incorporated into the hydrophobic core of Peptide K_3. Both peptides showed good photoswitching behaviour, but azobenzene isomerization had only a moderate effect on coiled-coil interactions with binding partner E_3GY. The 340 nm irradiated (*cis* dominant) state of **K_3-APhe1** showed a 1.3-fold decrease in K_f compared to the dark (trans dominant) state. Peptide **K_3-APhe2** showed the opposite behaviour, increasing the K_f by 1.5-fold, which can be attributed to the repulsion between the glutamic acid side chains and the carboxylic acid group of **APhe2**. A novel azobenzene amino acid, **APgly**, was synthesized based on L-phenylglycine and showed effective photoswitching between the *cis* and *trans* states as the Fmoc-protected amino acid in MeCN. When incorporated in peptide

K_3, **APgly** also showed stability to photocycling under aqueous conditions, and exhibited a 1.6-fold slower relaxation from the 340 nm PSS. CD experiments demonstrated a difference in folding between the dark and irradiated states, and thermal melting experiments revealed a coiled-coil K_f that was reduced 4.65-fold after isomerization with 340 nm light. Combined with the highest overall K_f in the dark state, **APgly** is the superior amino acid for coiled-coil photoswitching compared to both phenylalanine derivatives.

To better understand the interactions of the azobenzene amino acid in the coiled coil, MD simulations of **K_3-APhe1** and **K_3-APgly** with binding partner E_3 were performed. These simulations showed more distance changes between the *cis* and *trans* isomers of **APhe1** than was observed for **APgly**, indicative of a rearrangement of the amino acid after isomerization. Positioning of the **APgly** diazene group close to the centre of the hydrophobic coiled-coil interface, combined with less rearrangement of the azobenzene after isomerization makes **APgly** the more effective photoswitch for functional coiled-coil motifs and assemblies.

5.4 Methods

Fmoc-protected amino acids and fmoc chloride were purchased from Novabiochem (Amsterdam, The Netherlands). Acetic anhydride (Ac_2O), acetonitrile (MeCN), dimethylformamide (DMF), piperidine, pyridine, $NaHCO_3$, trifluoroacetic acid (TFA) and tetrahydrofuran (THF) were purchased from Biosolve (Valkenswaard, The Netherlands). Oxyma pure was purchased from Carl Roth (Karlsruhe, Germany). Acetic acid (AcOH), ammonia, ammonium chloride, ammonium formate, benzophenone imine, 2,2'-Bis(diphenylphosphino)-1,1'-binaphthalene (*rac*-BINAP), 1,2-bis(2-mercapto-ethoxy)-ethane (EDDT), cesium carbonate, di-*tert*-butyl decarbonate (Boc_2O), fmoc-4-nitro-L-phenylalanine, 4-hydroxy-L-phenylglycine, lithium hydroxide, nitrosobenzene, *N*-*N*'-diisopropylcarbodiimide (DIC), oxone, palladium acetate, palladium on carbon (Pd/C, 10%), L-phenylalanine, tert-butyl 4-aminobenzoate, thionyl chloride, triethylamine (TEA), trifluoromethanesulfonic anhydride (Tf_2O) and zinc powder were purchased from Sigma Aldrich (Zwijndrecht, The Netherlands). Chloroform, dichloromethane (DCM), diethyl ether (Et_2O), ethyl acetate (EtOAc), ethanol (EtOH), methanol (MeOH), pentane, petroleum ether (PE), sodium sulfate and toluene were supplied by Honeywell (Meppel, The Netherlands). All reagents were used as purchased. Ultrapure water was purified using a Milli-Q™ purification system from Millipore (Amsterdam, The Netherlands).

Peptide synthesis was performed via Fmoc-based SPPS, on a CEM Liberty Blue microwave-accelerated peptide synthesizer. Peptides were prepared on a 0.1 mmol scale using Tentagel S RAM resin (0.22 mmol/g). 5 equivalents each of amino acid, Oxyma pure and DIC, the latter two of which were coupling reagents were heated at 90 °C for 4 minutes to facilitate coupling. Deprotection was achieved with 20% piperidine in DMF heated to 90 °C for 1 minute. Between deprotection and peptide coupling 3 DMF washes were performed, with a single washing step between the coupling and deprotection steps. Azobenzene amino-acids **2**, **3** and **10** were coupled manually, using 2.5 equivalents of amino acid, 2.5 equivalents of HATU and 5 equivalents DIPEA in DMF for 2-3 hours. After the last Fmoc deprotection, the N-terminus was acylated using 5 mL/mmol each of Ac_2O and pyridine in DMF, for 5 minutes. The resin was washed 3 times with DMF, MeOH and DCM followed by air-drying. Cleavage of peptide was achieved performed with TFA (8 mL) containing 2.5% water and 2.5% TIS for 1 hour, followed by precipitation of the product in Et_2O. The product was collected via centrifugation (4000 rpm, 10 minutes), the organic layer removed and the product resuspended in water for direct purification or lyophilization.

Peptides were purified using reverse-phase HPLC on a Shimadzu system consisting of two KC-20AR pumps and an SPD-20A or SPD-M20A detector fitted with a 21.2x150 mm Phenomenex Kinetix Evo C18 column. A nonlinear gradient from 10-90% MeCN in water was used, with 0.1% TFA as the ion-pair reagent, at a flow rate of 12 ml/min. Collected fractions were checked via analytical HPLC, pooled and lyophilized twice to yield the dry products. MS characterization of purified peptides can be found in **Table S5.4**.

Analytical methods

LC-MS analysis was performed on a Thermo Scientific TSQ quantum access MAX mass detector connected to an Ultimate 3000 liquid chromatography system fitted with a 50x4.6 mm Phenomenex Gemini 3 µm C18 column. LC-MS spectra were recorded using a linear gradient of 10%-90% MeCN in H_2O + 0.1% TFA.

Analytical HPLC was performed using a Shimadzu Prominence-*i* LC-2030C 3D system fitted with a 4.6x50 mm Phenomenex Kinetix Evo C18 column. The isomeric ratio of **10** was quantified using a linear gradient of 10-90% MeCN in water containing 0.1% TFA as buffer. For each measurement, 2 µL of a 200 mM solution of **10** was injected, and measurements were repeated 3 times for accuracy.

UV-Vis spectra were measured on an Agilent Cary-300 spectrophotometer fitted with an Agilent temperature controller. Spectra were measured at 20 °C in a 1 cm quartz low-volume cuvette, using a scanning speed of 200 nm/min. Spectra were baseline corrected using a blank measurement with the same solvent used for sample preparation.

CD spectra were recorded on a Jasco J-815 CD spectrometer fitted with a Peltier temperature controller. Spectra were record in a 2 mm quartz cuvette at 20 °C using either PBS or low-salt buffer (2 mM NaCl, 10 mM phosphate) at pH 7.4. Spectra were recorded between 190 and 280 nm with 1 nm intervals, at a scan rate of 100 nm/min with 5 subsequent spectra averaged to minimize noise. The mean residue molar ellipticity (θ, deg cm^2 $dmol.res^{-1}$), was calculated using equation 1:

$$[\theta] = (100 * [\theta]_{obs})/(c * n * l) \qquad (1)$$

Where $[\theta]_{obs}$ represents the observed ellipticity in mdeg, *c* represents the peptide concentration in mM, *n* the number of peptide bonds and *l* the path length of the cuvette in cm. Thermal melting curves were generated by recording θ_{222nm} between 5 and 90 °C, at a speed of 1 °C/min. If irradiated samples were used, samples were reilluminated every 30 minutes. Melting curves were measured at 4 different concentrations and fitted using the Fitdis software package.[27]

Sample illumination at 340 nm was achieved using a Thorlabs M340F3 Fiber-coupled LED powered by a T-Cube driver at 1000 mA. For all other wavelengths, high-power single chip LEDs were purchased from Roithner Laser (Vienna, Austria) from the H2A1 series. LEDs from Roithner Laser were mounted on an aluminum back plate for heat dissipation, and powered at 350 mA current using a driver built in-house. For illumination the LED was placed parallel to the side of the cuvette at a distance of 5 mm, and centered to the width and height of the sample.

Molecular simulations

Geometry Optimization: Input geometries of the amino acids for the MD simulations were obtained by geometry optimization performed using the Amsterdam Density Functional (ADF2019.302)[33-35] software package, using the BLYP functional with D3(BJ) dispersion correction,[36, 37] and a TZ2P basis set, which is of triple-ζ quality for all atoms and has been improved by two sets of polarization functions. The accuracies of the fit scheme (Zlm fit) and the integration grid (Becke

grid) were set to VERYGOOD. All structures were verified to be at the stationary point by the absence of negative frequencies.

Force field parametrization: A new atom type NX was introduced to the AMBER-96 force field[38] for the diazo nitrogen atoms in **APgly** and **APhe1**. Bond lengths, angles and dihedral angles for this new atom type were derived from DFT calculated optimized geometries, and are displayed in **table S5.3**. Force constants from similar existing atom type combinations were adapted. For the production runs, a high force constant (1000 kJ mol^{-1} rad^{-2}) was used to restrain the cis/trans dihedral angle.

System setup: The NMR structure of the E_3/K_3 coiled-coil heterodimer was retrieved from the protein data bank (PDB, ID: 1U0I).[32] Ile9 of peptide K was mutated manually to **APgly** or **APhe1** and solvated with TIP3P water[39] in a 5x5x5 nm^3 simulation box. After steepest descent energy minimization, the system was equilibrated for 500 ps with and, subsequently, without position restraints on the protein atoms. For each system, three independent production runs of 500 ns were performed with pseudorandom initial velocities.

Simulation details: All molecular dynamics (MD) simulations were performed with GROMACS 2019.3.[40] A 1 fs time step was used. Constant temperature (300K, τ_T = 0.1 ps) and pressure (1 bar, τ_P = 2 ps) were maintained by the velocity rescaling thermostat[41] and the Berendsen barostat,[42] respectively. The system's compressibility was set to $4.5 \cdot 10^{-5}$ bar^{-1}. Neighbour lists were recalculated every 100 steps with a cut-off of 1 nm using the Verlet cut-off scheme.[43] Particle-mesh Ewald (PME)[44] electrostatics (0.11 nm grid) and Van der Waals interactions are shifted such that they switch off at the cut-off distance (1 nm)

Organic Synthesis

Protocol A, general method for the reduction of nitrophenylalanine: Fmoc-4-nitro-L-phenylalanine was dissolved in absolute EtOH (150 mL/g), combined with ammonium chloride (5 eq.) and Zn dust (4 eq.), and the reaction refluxed for 2 hours. After evaporation of solvent, the resulting solids were combined with EtOAc and excess 1 M HCl, the phases separated and the aqueous layer extracted twice with ethyl acetate. The two organic layers were combined, washed with deionized water, and dried with anhydrous Na_2SO_4. Solvent was evaporated under reduced pressure, yielding Fmoc-(4-amino)-L-phenylalanine that was used without further purification.

4-tert-Butyl-nitrosobenzoate: 4-Amino tert-butyl benzoate (765 mg, 3.96 mmol) was dissolved in 10 mL DCM and combined with Oxone (1263 mg, 8.29 mmol) in 13 mL H_2O, and the mixture was stirred vigorously under reflux for 20 hours. The layers were separated, and the aqueous layer extracted with an additional 20 mL DCM. The combined organic layers were washed sequentially with 10 mL 1M HCl, 10 mL half-saturated $NaHCO_3$ and 10 mL brine, dried over Na_2SO_4, and solvent was removed to yield the crude product. The product was purified via column chromatography (Et_2O/C_5H_{12}) to yield 220 mg of the product as bright green needles (1.06 mmol, 27%) that were used directly in the Mills reaction. **^{1}H NMR** (500 MHz, $CDCl_3$) δ 8.23 (d, *J* = 8.7 Hz, 2H), 7.91 (d, 2H), 1.62 (s, 9H). **^{13}C NMR** (126 MHz, $CDCl_3$) δ 164.78, 164.47, 137.28, 130.94, 130.65, 123.51, 120.47, 82.53, 28.25.

N-Fmoc-4-nitro-L-phenylalanine (1): To a solution of L-phenylalanine (4.96 g, 30 mmol) dissolved in H_2SO_4 (95%, 22.5 mL) and cooled over ice was added 4.2 mL nitrating solution (prepared by mixing 2.8 mL of 60% HNO_3 and 2.2 mL 95% H_2SO_4 on ice) dropwise over 3.5 hours. The solution was neutralized with ammonia solution (25%) added dropwise until pH 6 was achieved and precipitate observed. The precipitate was collected by filtration and washed with 5 x 30 mL water. After drying, 3.5 g (55%) of 4-nitrophenylalanine was collected as an off-white solid. This intermediate (1.05 g, 5.00 mmol) was dissolved in a mixture of 20 mL 0.5 M Na_2CO_3, 13 mL acetone, 13 mL deionized water and 49.6 mg dodecyl sulfate and cooled over ice. A solution of Fmoc-chloride (1.32 g, 5.1 mmol) in 10 mL acetone was added dropwise to the reaction, and it was left to stir overnight at room temperature. The reaction was quenched by dilution into 300 mL cold water and addition of 5 mL, 2 M HCl. The precipitate was filtered and redissolved in 100 mL, 0.5 M Na_2CO_3. The mixture was allowed to stir at 70 °C for 1 hour, after which the white precipitate was filtered out and the filtrate was collected and acidified to pH < 3 with 2 M HCl. The precipitate was collected and dried to yield 1.5 g of a white solid (69%, 38% over two steps). **^{1}H NMR** (400 MHz, DMSO-d6) 8.15 (d, 2H), 7.89 (d, J = 7.6 Hz, 2H), 7.80 (d, J = 8.7 Hz, 1H), 7.62 (dd, J = 7.5, 2.7 Hz, 2H), 7.56 (d, J = 8.5 Hz, 2H), 7.41 (t, J = 7.4 Hz, 2H), 7.30 (q, J = 7.4 Hz, 2H), 4.32 – 4.13 (m, 4H), 3.25 (dd, J = 13.8, 4.4 Hz, 1H), 3.02 (dd, J = 13.8, 10.8 Hz, 1H). **LC-MS** RT = 7.57 min, m/z= 178.47 (calc Fm^+ = 179.09), 454.61 (calc [**1** + Na^+]$^+$ = 455.12), 470.00 (calc [**1** + K^+]$^+$ = 471.10).

Preparation of N-fmoc-(4-phenylazo)-L-phenylalanine, APhe1 (2): Fmoc-4-nitrophenylalanine (1.34 g, 3.11 mmol) was reduced according to protocol A (see above), resulting in 1.04 g crude Fmoc-4-aminophenylalanine. The intermediate

was dissolved in 60 mL AcOH, before nitrosobenzene (350 mg, 3.27 mmol, 1.25 eq.) dissolved in 5 mL AcOH was added and the solution left for 20 hours. The product was precipitated by addition of the reaction mixture to 250 mL H_2O, and collected via filtration. The crude product was redissolved in EtOAc, dried with Na_2SO_4, filtered and solvent evaporated. The solids were purified via column chromatography (dry loading, DCM/MeOH + 0.5% AcOH) and removal of solvents yielded 478 mg (0.97 mmol, 32% over 2 steps) of pure product as a brown powder. **^{1}H NMR** (500 MHz, DMSO-d6) 7.89 - 7.85 (m, 4H), 7.82 (d, J = 8.3 Hz, 3H), 7.66 - 7.54 (m,5H), 7.50 (d, J = 8.4 Hz, 2H), 7.38 (q, J = 7.9 Hz, 2H), 7.28 (dt, J = 14.9, 7.4 Hz, 2H), 4.30 - 4.24 (m,1H), 4.21 (d, J = 6.1 Hz, 2H), 4.19 - 4.13 (m, 1H), 3.21 (dd, J = 13.8, 4.4 Hz, 1H), 2.99 (dd, J = 13.8,10.7 Hz, 1H). **^{13}C NMR** (126 MHz, DMSO) 173.14, 155.96, 151.99, 150.65, 143.77, 143.71, 142.06, 140.69,140.68, 131.39, 130.24, 129.48, 127.61, 127.59, 127.05, 125.25, 125.19, 122.47, 120.10, 65.61, 55.22, 46.57, 36.32. **LC-MS** RT = 7.85 (cis), 8.90 (trans) min, m/z= 178.54 (calc Fm^+ = 179.09), 513.31 (calc [**2** + Na^+]$^+$ = 514.17).

Preparation of N-fmoc-L-(4-(4'-tert-Butoxycarbonyl)phenylazo)phenylalanine, (3): Fmoc-(4-nitro)-L-phenylalanine (2.02 mmol, 874 mg) was reduced according to general protocol A to yield 732 mg of Fmoc-(4-amino)-L-phenylalanine. The solids were dissolved by heating in 70 mL AcOH, and after it had returned to room temperature, 560 mg tert-Butyl-4-nitrosobenzoate was added (2.71 mmol) dissolved in 5 mL AcOH, and the reaction stirred for 20 h. Another 220 mg (1.06 mmol) of the nitrosobenzene was added to drive the reaction to completion, and the reaction stirred for another 20 h. The product was precipitated in 250 mL H_2O, collected via filtration, redissolved in acetone and the solvent was removed via rotary evaporation. The crude product was purified via column chromatography (PE/Et_2O + 1% AcOH) and solvent removed to yield 675 mg (1.14 mmol, 56% over two steps) of the pure product as a red semi-crystalline material. **^{1}H NMR** (400 MHz, $CDCl_3$): δ 8.12 (d, *J* = 8.5 Hz, 2H), 7.89 (dd, *J* = 11.5, 8.3 Hz, 4H), 7.76 (d, *J* = 7.6 Hz, 2H), 7.55 (d, *J* = 7.2 Hz, 2H), 7.39 (t, *J* = 7.4 Hz, 2H), 7.33 – 7.28 (m, 4H), 5.30 (d, *J* = 8.1 Hz, 1H), 4.83 – 4.71 (m, 1H), 4.51 – 4.47 (m, 1H), 4.39 (dd, *J* = 10.7, 6.8 Hz, 1H), 4.21 (t, *J* = 6.9 Hz, 1H), 3.26 (ddd, *J* = 45.1, 13.9, 5.8 Hz, 2H), 1.63 (s, 9H). **^{13}C NMR** (101 MHz, $CDCl_3$): δ 177.31, 165.40, 155.83, 154.93, 151.86, 143.84, 143.70, 141.47, 139.65, 133.84, 130.56, 130.38, 127.90, 127.23, 125.17, 125.11, 123.52, 122.63, 120.16, 81.71, 67.20, 54.58, 47.25, 37.82, 28.33. **LC-MS** RT = 8.79 (cis), 9.81 (trans) min, m/z= 178.47 (calc Fm^+ = 179.09), 591.25 (calc [**3** + H^+]$^+$ = 592.24), 613.35 (calc [**3** + Na^+]$^+$ = 614.23).

4-Hydroxy-L-phenylglycine methyl ester (4): Thionyl chloride (13.0 mL, 184 mmol, 9 eq.) was added dropwise to a suspension of 4-hydroxy-L-phenylglycine (3.39 g, 20.3 mmol) in 100 mL dry MeOH temperature controlled at 20 °C, over the course of 30 minutes. The clear solution was stirred overnight, and all liquid was evaporated under reduced pressure. The resulting oil was mixed with 50 mL Et_2O to yield an off-white precipitate, which was filtered and washed with 2x 50 mL Et_2O. The residue was dried under vacuum to yield 4.33 g of 4-hydroxy-phenylglycine methyl ester hydrochloride (19.9 mmol, 98%). **^{1}H NMR** (400 MHz, DMSO): δ 9.98 (s, 1H), 8.98 (s, 3H), 7.28 (d, *J* = 8.6 Hz, 2H), 6.84 (d, *J* = 8.6 Hz, 2H), 5.09 (s, 1H), 3.69 (s, 3H), 3.38 (s, 1H). **^{13}C NMR** (101 MHz, DMSO): δ 169.26, 158.60, 129.64, 122.61, 115.70, 54.90, 53.02.

N-Boc-4-hydroxy-L-phenylglycine methyl ester (5): A solution was prepared of 4-hydroxy-phenylglycine methyl ester (**4**, 1.11 g of the HCl salt, 5.11 mmol) in dry MeCN (70 mL) containing TEA (0.75 mL 5.39 mmol, 1.06 eq). Boc_2O (1.30 g, 5.96 mmol, 1.17 eq) was dissolved in 20 mL dry MeCN and added dropwise to the phenylglycine solution, and the solution stirred overnight. The solvent was evaporated and remaining solids redissolved in 50 mL DCM, which was subsequently washed with 25 mL 1M H_3PO_4, 50 mL H_2O and 25 mL brine. The organic layer was dried with Na_2SO_4 and the solvent evaporated. The crude product was purified via filtration through a plug of silica (eluent: EtOAc) and the solvent was removed to yield 1.33 g (4.71 mmol, 93%) of product as a white solid. **^{1}H NMR** (400 MHz, DMSO): δ 9.50 (s, 1H), 7.62 (d, *J* = 7.9 Hz, 1H), 7.20 – 7.13 (m, 2H), 6.75 – 6.65 (m, 2H), 5.05 (d, *J* = 7.9 Hz, 1H), 3.59 (s, 3H), 1.38 (s, 9H). **^{13}C NMR** (101 MHz, DMSO): δ 171.91, 157.25, 155.20, 129.10, 126.64, 115.19, 78.42, 57.10, 52.00, 28.19.

N-Boc-4-(trifluoromethanesulfonate)-L-phenylglycine methyl ester (6): N-boc-4-hydroxy-L-phenylglycine methyl ester (1.41 g, 5.02 mmol) was dissolved in 25 mL DCM and combined with 1 mL (7.5 mmol, 1.5 eq.) TEA. The reaction was cooled to -20 °C and Tf_2O (0.83 mL, 4.92 mmol, 0.98 eq.) was added in portions. After 30 minutes, the reaction was allowed to heat to room temperature and left to stir for 4 hours. The reaction was diluted with another 20 mL DCM and washed with 20 mL 0.5M HCl, 20 mL H_2O and 20 mL brine. The organic layer was dried over Na_2SO_4, the solvent was removed and the product purified over a silica column (Et_2O/C_5H_{12}) to yield 1.825 g of a clear oil (4.42 mmol, 98% yield relative to Tf_2O, 88% relative to **5**). The oil could be turned into a solid via dissolution in pentane and removal of the

solvent. **^{1}H NMR** (500 MHz, $CDCl_3$): δ 7.47 (d, *J* = 8.7 Hz, 2H), 7.30 – 7.23 (m, 2H), 5.77 – 5.61 (m, 1H), 5.37 (d, *J* = 7.2 Hz, 1H), 3.75 (s, 3H), 1.43 (s, 8H). **^{13}C NMR** (126 MHz, $CDCl_3$): δ 170.93, 154.76, 149.45, 137.93, 129.17, 121.92, 118.25(d, J_{CF} = 161 Hz), 80.72, 56.89, 53.21, 28.40, 27.80. **^{19}F NMR** (471 MHz, $CDCl_3$): δ -72.86.

N-Boc-4-((diphenylmethylene)-amino)-L-phenylglycine methyl ester (7): Cs_2CO_3 (460 mg, 1.4 mmol, 1.4 eq), N-Boc-(4-trifluoromethanesulfonate)-L-phenylglycine methyl ester (**6**, 413 mg, 1.03 mmol) and benzophenone imine (210 µL, 1.25 mmol, 1.21 eq) were placed in an oven-dried schlenck reaction vessel, and the flask was placed under a nitrogen atmosphere. $Pd(OAc)_2$ (15.5 mg, 0.07 mmol, 7%) and *rac*-BINAP (95 mg, 0.15 mmol, 15%) were combined in a separate vial, placed under nitrogen, and combined with 4 mL toluene and 2.5 uL H_2O (0.14 mmol, 14%) and heated to 85 °C. After 2 minutes the color of the catalyst solution had changed to bright red, transferred to the reaction flask and the reaction stirred at 100 °C for 20h. After cooling to RT, the liquid phase of the reaction was transferred to a separatory funnel, the solids washed 3x with 10 mL Et_2O, and this liquid also combined in the funnel. The organic layers were extracted with 2x 20 mL H_2O, dried with Na_2SO_4 and the solvent removed. The product purified over silica column (Et_2O/C_5H_{12}) and dried under high vacuum to yield 296 mg of a light-yellow solid (0.66 mmol, 65% yield). **^{1}H NMR** (500 MHz, $CDCl_3$): δ 7.72 (d, *J* = 7.0 Hz, 2H), 7.46 (t, *J* = 7.3 Hz, 1H), 7.39 (dd, *J* = 8.3, 6.8 Hz, 2H), 7.25 (d, *J* = 8.1 Hz, 4H), 7.14 – 7.07 (m, 4H), 6.69 (d, *J* = 8.4 Hz, 2H), 5.39 (d, *J* = 7.5 Hz, 1H), 5.19 (d, *J* = 7.5 Hz, 1H), 3.68 (s, 3H), 1.43 (s, 8H). **^{13}C NMR** (126 MHz, $CDCl_3$): δ 171.96, 168.66, 154.95, 151.54, 139.62, 136.07, 131.34, 130.97, 129.61, 129.47, 128.83, 128.34, 128.09, 127.56, 121.53, 80.21, 57.33, 52.65, 28.42.

N-Boc-(4-phenylazo)-L-phenylglycine methyl ester (8): Ammonium formate (1.1 g, 17.5 mmol, 15.8 eq.) and 10% Pd on carbon (50% water by weight, 125 mg, 5.8%) were combined with N-Boc-4-((diphenylmethylene)amino)-L-phenylglycine methyl ester (**7**, 496 mg, 1.11 mmol) under a nitrogen atmosphere. 4 mL MeOH was added and the reaction heated to 60 °C for 2h. The reaction was diluted with 10 mL DCM and filtered over celite, then washed with another 20 mL DCM. The organic layers were washed with 2x 30 mL H_2O, 1 x 10 mL brine, and dried over Na_2SO_4. The solvent was removed to yield 400 mg of an off-white solid. This was redissolved in 5 mL AcOH, and 167 mg (1.56 mmol, 1.4 eq) nitrosobenzene in 3 mL AcOH was added and the reaction stirred for 6 days. 50 mL DCM was added and the organic layer washed with 50 mL H_2O, 50 mL 3% NH_3 and 50 mL brine. The organic layer was dried

over dried over Na_2SO_4 and the solvent removed. The crude product was purified via column chromatography (Et_2O/C_5H_{12}) to yield 303 mg of an orange solid (0.82 mmol, 74%). **^{1}H NMR** (400 MHz, $CDCl_3$): δ 7.94 – 7.88 (m, 4H), 7.52 (m, 5H), 5.68 (d, *J* = 7.3 Hz, 1H), 5.41 (d, *J* = 7.3 Hz, 1H), 3.74 (s, 3H), 1.44 (s, 8H). **^{13}C NMR** (101 MHz, $CDCl_3$): δ 171.29, 152.73, 152.66, 139.84, 131.33, 129.25, 128.05, 123.45, 123.05, 80.51, 57.48, 53.06, 28.45.

N-fmoc-4-(phenylazo)-L-phenylglycine, Fmoc-APhe (10): To N-Boc-4-(phenylazo)-L-phenylglycine methyl ester (**9**, 311 mg, 0.84 mmol) dissolved in 6 mL THF was added 1M LiOH (1.26 mL, 1.5 eq.) and the reaction stirred for 90 minutes. After cooling the reaction was combined with 50 mL DCM and 50 mL 0.5 M HCl. The layers were separated, and the organic layer washed with 50 mL H_2O, 50 mL brine and dried over Na_2SO_4. The solvent was evaporated and the intermediate was redissolved in 5 mL DCM and 5 mL TFA was added. The reaction was stirred for 2 hours, after which the intermediate was precipitated in 100 mL cold Et_2O: C_5H_{12} and collected via centrifugation at 4000 rpm for 10 minutes. The precipitate was dried under a stream of air for 5 minutes, then suspended in 150 mL 25% H_2O/THF. $NaHCO_3$ (1.5 g) was added to neutralize the solution and Fmoc-chloride (258 mg, 1 mmol, 1.19 eq.) dissolved in 6 mL THF was added to the reaction dropwise. The solution was stirred overnight, and the next day all THF was evaporated. The reaction was combined with 60 mL DCM and 100 mL 1M HCl and separated. The Aqueous layer was extracted with 40 mL DCM, organic layers combined and washed with 100 mL H_2O, 50 mL brine and dried over Na_2SO_4. The solvent was removed and the remaining solids purified via column chromatography (DCM/MeOH with 0.5 % AcOH) to yield 254 mg of product as a bright orange powder (0.3 mmol, 63% over 3 steps). **^{1}H NMR** (600 MHz, DMSO): δ 13.11 (s, 1H), 8.44 – 8.31 (m, 1H), 7.93 – 7.87 (m, 6H), 7.77 (d, *J* = 7.5 Hz, 2H), 7.66 (d, *J* = 8.5 Hz, 2H), 7.64 – 7.55 (m, 3H), 7.44 – 7.39 (m, 2H), 7.32 (dt, *J* = 11.7, 7.5 Hz, 2H), 5.32 (d, *J* = 8.2 Hz, 1H), 4.34 – 4.22 (m, 3H). **^{13}C NMR** (151 MHz, DMSO): δ 171.68, 155.91, 151.92, 151.50, 143.84, 143.77, 140.74, 140.66, 131.71, 129.55, 128.99, 127.70, 127.11, 125.42, 125.42, 122.64, 120.15, 66.01, 57.78, 46.62. **LC-MS** RT = 6.65 (cis), 8.80 (trans) min, m/z= 178.54 (calc Fm^+ = 179.09), 238.71 (calc [**10** + $2H^+]^{2+}$ = 239.59), 477.28 (calc [**10** + $H^+]^+$ = 478.17), 499.46 (calc [**10** + $Na^+]^+$ = 500.16).

5.5 References

1. Kumita, J. R., Smart, O. S., and Woolley, G. A. (**2000**) Photo-control of helix content in a short peptide. *P. Natl. Acad. Sci. USA 97*, 3803-3808.

2. Wagschal, K.*, et al.* (**1999**) The role of position a in determining the stability and oligomerization state of α-helical coiled coils: 20 amino acid stability coefficients in the hydrophobic core of proteins. *Protein Sci. 8*, 2312-2329.

3. Tripet, B.*, et al.* (**2000**) Effects of side-chain characteristics on stability and oligomerization state of a de Novo-designed model coiled-coil: 20 amino acid substitutions in position "d". *J. Mol. Biol. 300*, 377-402.

4. Acharya, A.*, et al.* (**2002**) A Heterodimerizing Leucine Zipper Coiled Coil System for Examining the Specificity of a Position Interactions: Amino Acids I, V, L, N, A, and K. *Biochem. 41*, 14122-14131.

5. Acharya, A., Rishi, V., and Vinson, C. (**2006**) Stability of 100 Homo and Heterotypic Coiled−Coil a−a' Pairs for Ten Amino Acids (A, L, I, V, N, K, S, T, E, and R). *Biochem. 45*, 11324-11332.

6. Zhu, H.*, et al.* (**2000**) The contribution of buried polar groups to the conformational stability of the GCN4 coiled coil11Edited by C. R. Matthews. *J. Mol. Bio. 300*, 1377-1387.

7. Fletcher, J. M.*, et al.* (**2017**) N@a and N@d: Oligomer and Partner Specification by Asparagine in Coiled-Coil Interfaces. *ACS Chem. Biol. 12*, 528-538.

8. García-Echeverría, C. (**1996**) Disruption of coiled coil formation by methionine oxidation. *Bioorg. Med. Chem. Lett. 6*, 229-232.

9. Zimenkov, Y.*, et al.* (**2006**) Rational Design of a Reversible pH-Responsive Switch for Peptide Self-Assembly. *J. Am. Chem. Soc. 128*, 6770-6771.

10. Dublin, S. N., and Conticello, V. P. (**2008**) Design of a Selective Metal Ion Switch for Self-Assembly of Peptide-Based Fibrils. *J. Am. Chem. Soc. 130*, 49-51.

11. Boyle, A. L.*, et al.* (**2019**) Selective coordination of three transition metal ions within a coiled-coil peptide scaffold. *Chem. Sci. 10*, 7456-7465.

12. Goodman, M., and Kossoy, A. (**1966**) Conformational Aspects of Polypeptide Structure. XIX. Azoaromatic Side-Chain Effects1,2. *J. Am. Chem. Soc. 88*, 5010-5015.

13. Bose, M.*, et al.* (**2006**) The Incorporation of a Photoisomerizable Amino Acid into Proteins in E. coli. *J. Am. Chem. Soc. 128*, 388-389.

14. Nakayama, K., Endo, M., and Majima, T. (**2005**) A Hydrophilic Azobenzene-Bearing Amino Acid for Photochemical Control of a Restriction Enzyme BamHI. *Bioconjugate Chem. 16*, 1360-1366.

15. Nakayama, K., Endo, M., and Majima, T. (**2004**) Photochemical regulation of the activity of an endonuclease BamHI using an azobenzene moiety incorporated site-selectively into the dimer interface. *Chem. Commun.*, 2386-2387.

16. John, A. A.*, et al.* (**2015**) Synthesis and Site-Specific Incorporation of Red-Shifted Azobenzene Amino Acids into Proteins. *Org. Lett. 17*, 6258-6261.

17. Luo, J.*, et al.* (**2018**) Reversible and Tunable Photoswitching of Protein Function through Genetic Encoding of Azobenzene Amino Acids in Mammalian Cells. *Chembiochem : a European journal of chemical biology 19*, 2178-2185.

18. Kneuttinger, A. C.*, et al.* (**2019**) Light Regulation of Enzyme Allostery through Photo-responsive Unnatural Amino Acids. *Cell. Chem. Bio. 26*, 1501-1514.e9.

19. Hoppmann, C.*, et al.* (**2011**) Photoswitchable Click Amino Acids: Light Control of Conformation and Bioactivity. *Chembiochem : a European journal of chemical biology 12*, 2555-2559.

20. Hoppmann, C.*, et al.* (**2015**) In Situ Formation of an Azo Bridge on Proteins Controllable by Visible Light. *J. Am. Chem. Soc. 137*, 11218-11221.

21. Wu, Y. Y., and Collier, J. H. (**2017**) alpha-Helical coiled-coil peptide materials for biomedical applications. *WIREs Nanomed Nanobiotechnol. 9*, e1424.

22. Utterström, J.*, et al.* (**2021**) Coiled coil-based therapeutics and drug delivery systems. *Adv. Drug Del. Rev 170*, 26-43.

23. Szilák, L., Moitra, J., and Vinson, C. (**1997**) Design of a leucine zipper coiled coil stabilized 1.4 kcal mol-1 by phosphorylation of a serine in the e position. *Protein Sci. 6*, 1273-83.

24. Winter, D. L.*, et al.* (**2020**) Design of Tunable Protein Interfaces Controlled by Post-Translational Modifications. *ACS Synth. Biol. 9*, 2132-2143.

25. Robson Marsden, H.*, et al.* (**2009**) A Reduced SNARE Model for Membrane Fusion. *Angew. Chem. Int. Edit. 48*, 2330-2333.

26. Litowski, J. R., and Hodges, R. S. (**2002**) Designing heterodimeric two-stranded alpha-helical coiled-coils - Effects of hydrophobicity and alpha-helical propensity on protein folding, stability, and specificity. *J. Biol. Chem. 277*, 37272-37279.

27. Rabe, M.*, et al.* (**2015**) Determination of Oligomeric States of Peptide Complexes Using Thermal Unfolding Curves. *Biopolymers 104*, 65-72.

28. Davies, A. J., Ashwood, M. S., and Cottrell, I. F. (**2000**) A Facile Synthesis of Substituted Phenylglycines. *Syn. Commun. 30*, 1095-1102.

29. Lee, D.-Y., and Hartwig, J. F. (**2005**) Zinc Trimethylsilylamide as a Mild Ammonia Equivalent and Base for the Amination of Aryl Halides and Triflates. *Org. Lett. 7*, 1169-1172.

30. Wolfe, J. P.*, et al.* (**1997**) An Ammonia Equivalent for the Palladium-Catalyzed Amination of Aryl Halides and Triflates. *Tetrahedron lett. 38*, 6367-6370.

31. Asano, T., and Okada, T. (**1984**) Thermal Z-E isomerization of azobenzenes. The pressure, solvent, and substituent effects. *J. Org. Chem. 49*, 4387-4391.

32. Lindhout, D. A.*, et al.* (**2004**) NMR solution structure of a highly stable de novo heterodimeric coiled-coil. *Biopolymers 75*, 367-375.

33. Zozulia, O., Dolan, M. A., and Korendovych, I. V. (**2018**) Catalytic peptide assemblies. *Chem. Soc. Rev. 47*, 3621-3639.

34. te Velde, G.*, et al.* (**2001**) Chemistry with ADF. *J. Comp. Chem. 22*, 931-967.

35. Fonseca Guerra, C.*, et al.* (**1998**) Towards an order-N DFT method. *Theor. Chem. Acc. 99*, 391-403.

36. Grimme, S*., et al.* (**2010**) A consistent and accurate ab initio parametrization of density functional dispersion correction (DFT-D) for the 94 elements H-Pu. *J. Chem. Phys. 132*, 154104.

37. Grimme, S., Ehrlich, S., and Goerigk, L. (**2011**) Effect of the damping function in dispersion corrected density functional theory. *J. Comp. Chem. 32*, 1456-1465.

38. Kollman, P*., et al.* (**1997**) The development/application of a 'minimalist' organic/biochemical molecular mechanic force field using a combination of ab initio calculations and experimental data, in *Computer Simulation of Biomolecular Systems: Theoretical and Experimental Applications* (van Gunsteren, W. F., Weiner, P. K., and Wilkinson, A. J., Eds.) pp 83-96, Springer Netherlands, Dordrecht.

39. Jorgensen, W. L*., et al.* (**1983**) Comparison of simple potential functions for simulating liquid water. *J. Chem. Phys. 79*, 926-935.

40. Abraham, M. J*., et al.* (**2015**) GROMACS: High performance molecular simulations through multi-level parallelism from laptops to supercomputers. *SotwareX 1-2*, 19-25.

41. Bussi, G., Donadio, D., and Parrinello, M. (**2007**) Canonical sampling through velocity rescaling. *J. Chem. Phys. 126*, 014101.

42. Berendsen, H. J. C*., et al.* (**1984**) Molecular dynamics with coupling to an external bath. *J. Chem. Phys. 81*, 3684-3690.

43. Verlet, L. (**1967**) Computer "Experiments" on Classical Fluids. I. Thermodynamical Properties of Lennard-Jones Molecules. *Phys. Rev. 159*, 98-103.

44. Darden, T., York, D., and Pedersen, L. (**1993**) Particle mesh Ewald: An N·log(N) method for Ewald sums in large systems. *J. Chem. Phys. 98*, 10089-10092.

Supporting information for Chapter 5

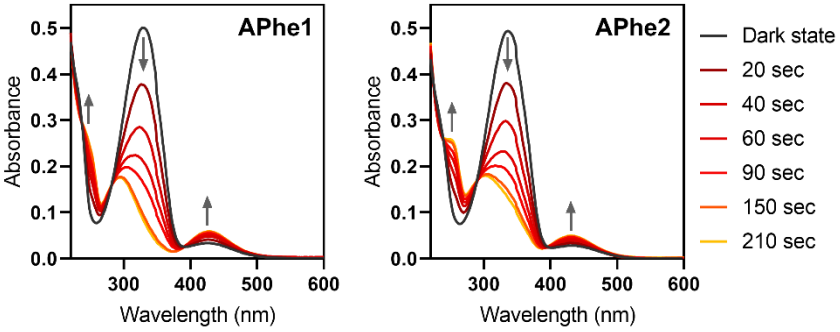

Figure S5.1: UV-Vis spectra of peptide K_3 containing either APhe1 or APhe2 at different time intervals during illumination with 340 nm light. Measurements were performed at 20 °C in PBS with [peptide] = 50 µM. Arrows indicate direction of change after illumination.

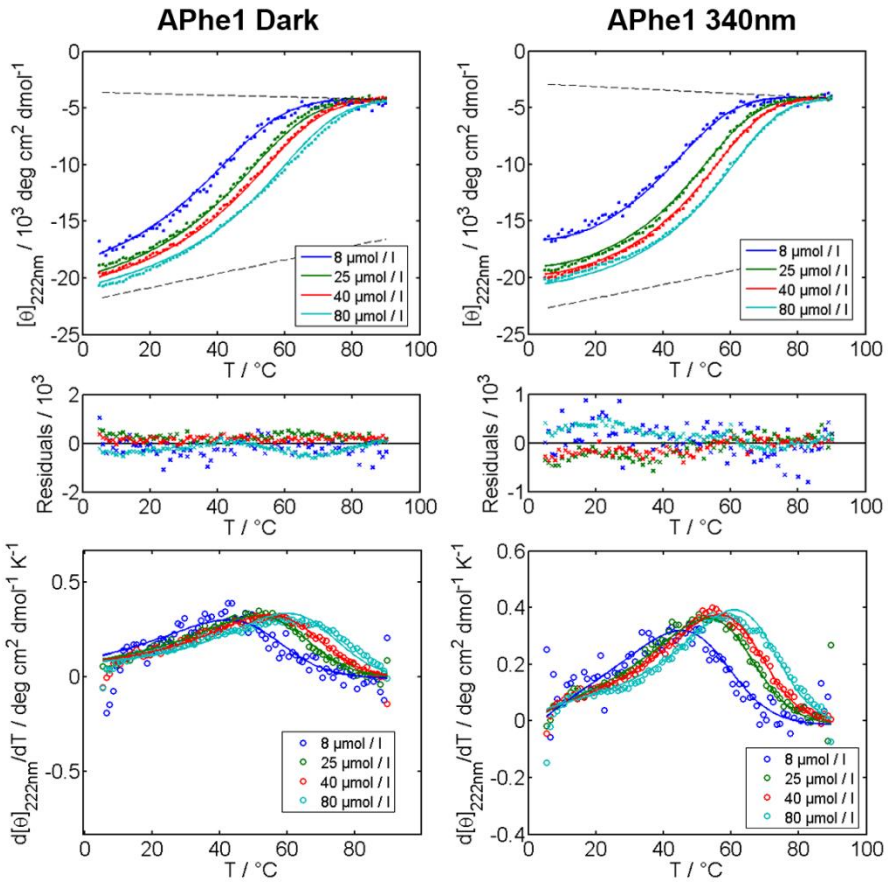

Figure S5.2: Fitting of CD melting curves (top) for peptide K_3-APhe1 with E_3GY in the dark adapted (left) and 340 nm irradiated (right) states performed using the Fitdis software program. Residuals (middle) and derivatives (bottom) of the best fitting (dimeric) model are shown. Measurements were performed in PBS.

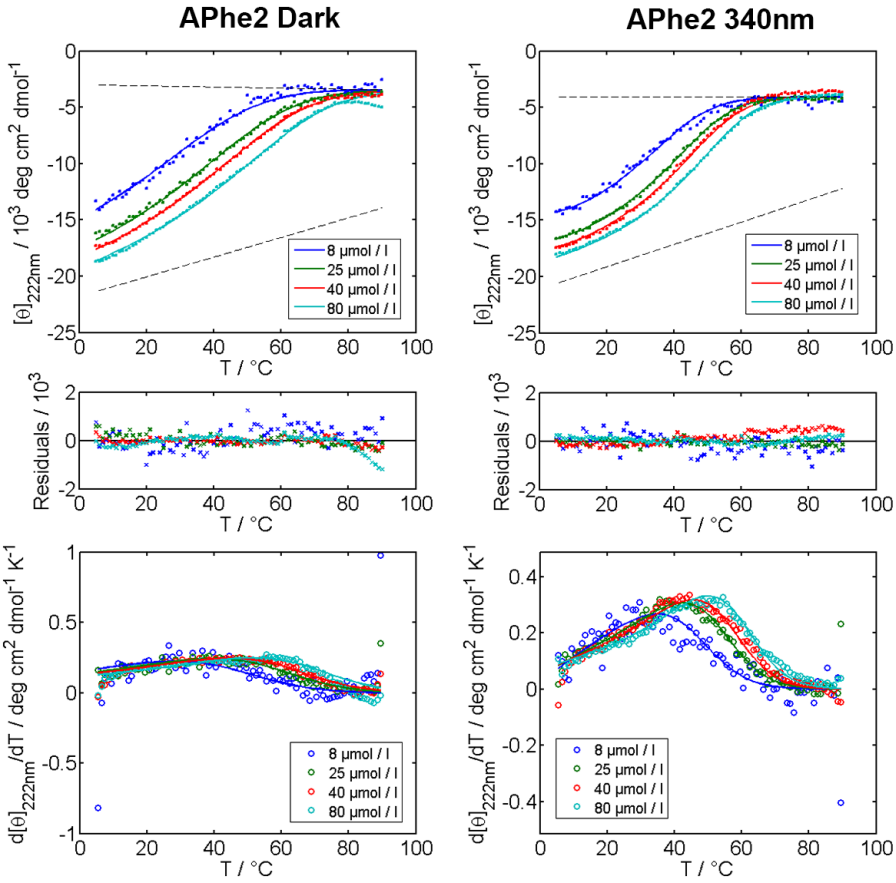

Figure S5.3: Fitting of CD melting curves (top) for peptide K_3-APhe2 with E_3GY in the dark adapted (left) and 340 nm irradiated (right) states performed by the Fitdis software program. Residuals (middle) and derivatives (bottom) of the best fitting (dimeric) model are shown. Measurements were performed in PBS.

Table S5.1: Fit results of thermal unfolding curves for K_3 peptides containing azophenylalanine amino acids with binding partner E_3GY, in either the dark adapted or 340 nm irradiated state.

Coiled-coil system	K_3-APhe1 Dark	K_3-APhe1 340 nm	K_3-APhe2 dark	K_3-APhe2 340 nm
$\Delta H°^a$ (kJ mol^{-1})	224.7 ± 12.4	261.4 ± 7.4	175.0 ± 12.1	259.0 ± 9.7
$T°^b$ (°C)	123 ± 3.1	114.1 ± 1.5	142.5 ± 5.4	102.1 ± 2.1
ΔC_p (kJ mol^{-1} k^{-1})	1.69 ± 0.22	2.46 ± 0.15	1.07 ± 0.17	2.65 ±0.22
θ_F (deg cm^2 dmol^{-1})	-22,067 ± 413	-23,009 ± 358	-21,790 ± 548	-21,112 ± 447
m_F	61.3 ± 16.7	59.9 ± 14.03	87.2 ± 27.1	99.1 ± 20.6
θ_u (deg cm^2 dmol^{-1})	-3,566 ± 1062	-2,830 ± 876	-2,986 ± 887	-4,078 ± 545
m_u	-7.4 ± 13.0	-15.0 ± 10.7	-5.0 ± 11.0	0.0 ± 7.0
$\Delta G_{20}{}^c$ (kJ mol^{-1})	33.5	32.8	29.97	30.94
$\Delta S_{20}{}^c$ (J mol^{-1} k^{-1})	57	-8.95	46.31	36.7
$\Delta H_{20}{}^c$ (kJ mol^{-1})	50.23	30.21	43.54	41.70
$K_f{}^c$ (M^{-1}, 20 °C)	9.19 10^5	7.09 10^5	2.18 10^5	3.26 10^5
$K_u{}^c$ (µM, 20 °C)	**1.09**	**1.41**	**4.58**	**3.07**
Dark/340nm PSS		1.30		0.67
Adjusted R^2	0.997	0.998	0.996	0.997
RMSE	300.1	248.2	298.9	248.5

[a] $\Delta H°$ and T° are the enthalpy and the temperature where $\Delta G = 0$ and $K_U = K_F = 1$. [b] ΔC_P is the change in heat capacity upon unfolding. [c] Binding model at 20 (°C).

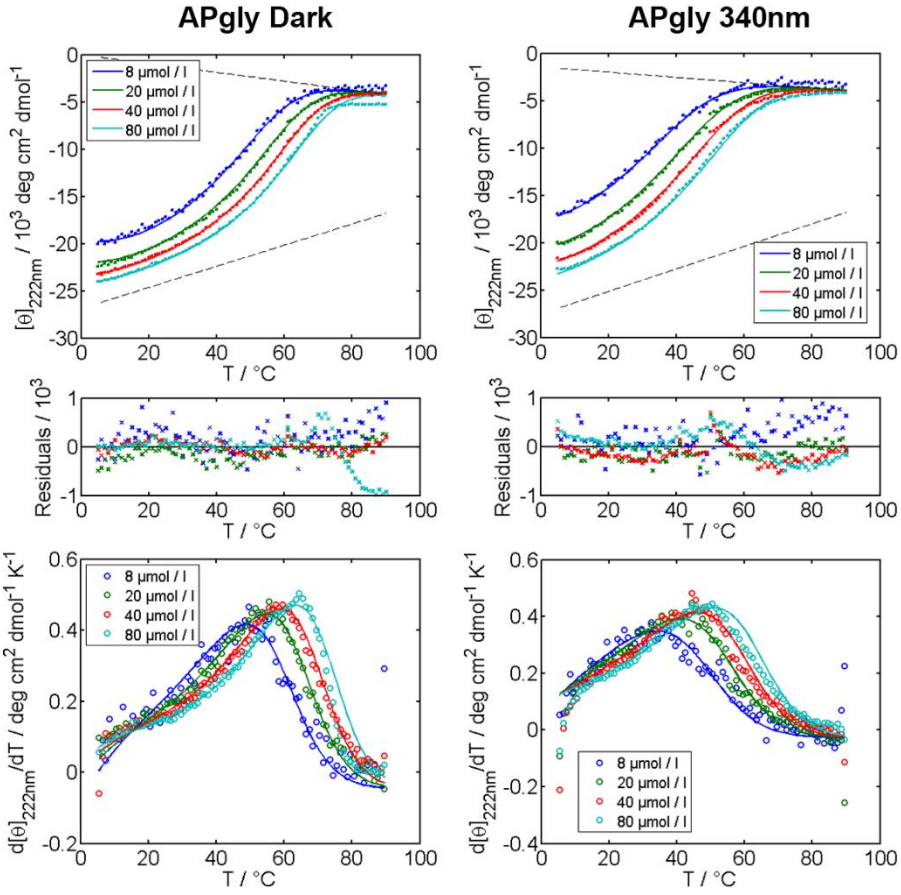

Figure S5.4: Fitting of CD melting curves (top) for peptide K_3-APgly with E_3GY in the dark adapted (left) and 340 nm irradiated (right) states performed by the Fitdis software program. Residuals (middle) and derivatives (bottom) of the best (dimeric) fitting model are shown. Measurements were performed in PBS.

Table S5.2: Fit results of thermal unfolding curves for K_3 peptides containing azophenylglcyine with coiled-coil binding partner E_3GY, in either the dark adapted or 340 nm irradiated state

Coiled-coil system	**K_3-APgly dark**	**K_3-APgly 340 nm**
$\Delta H°$[a] (kJ mol^{-1})	285.2 ± 6.5	236 ± 7.1
T°[b] (°C)	113 ± 1.2	110.5 ± 1.9
ΔC_p (kJ mol^{-1} k^{-1})	2.8 ± 0.13	2.15 ± 0.14
θ_F (deg cm^2 dmol^{-1})	-26877 ± 353	-27513 ± 520
m_F	112 ± 12.6	119 ± 23.9
θ_u (deg cm^2 dmol^{-1})	0 ± 1153	-1424 ± 687
m_u	-46.6 ± 13.9	-28 ± 8.7
ΔG_{20}[c] (kJ mol^{-1})	34.5	30.7
ΔS_{20}[c] (J mol^{-1} k^{-1})	-33	37.9
ΔH_{20}[c] (kJ mol^{-1})	24.8	41.8
K_f[c] (M^{-1}, 20 °C)	1.38 10^6	2.97 10^5
K_u[c] (µM, 20 °C)	**0.72**	**3.37**
Dark/340nm PSS		4.65
Adjusted R^2	0.998	0.998
RMSE	274.3	288.7

[a] $\Delta H°$ and T° are the enthalpy and the temperature where $\Delta G = 0$ and $K_U = K_F = 1$. [b] ΔC_P is the change in heat capacity upon unfolding. [c] Binding model at 20 (°C).

MD simulations

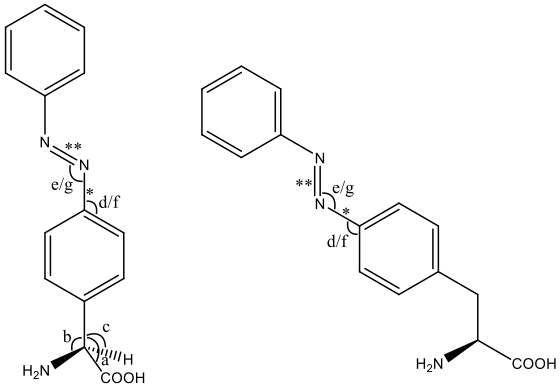

Table S5.3: Bond lengths, angles and dihedral angles for new atom types required for the integration of **APgly** (top left) and **APhe1** (top right) into the AMBER-96 force field for molecular dynamics simulations of azobenzene-amino acids. Bond lengths and angles as computed at BLYP-D3(BJ)/TZ2P.

	Bond type	**Residue**	**Bond length (nm)**	**Force constant (kJ mol^{-1} nm^{-1})**	**Adapted from**
*	CA-NX	All	0.14398	357313.6	CA-NA
**	NX-NX	All	0.14354	357313.6	CA-NA

	Angle type	**Residue**	**Angle (degrees)**	**Force constant (kJ mol^{-1} rad^{-1})**	**Adapted from**
a	CA-CT-C	Diazophenylglycine	109.139	527.184	CA-CT-CT
b	CA-CT-N	Diazophenylglycine	110.762	527.184	C-CT-N
c	CA-CT-H1	Diazophenylglycine	108.439	418.400	CA-CT-HC
d	CA-CA-NX	Cis	119.225	585.760	NA-CN-NC
e	CA-NX-NX	Cis	121.626	585.760	NA-CN-NC
f	CA-CA-NX	Trans	121.615	585.760	NA-CN-NC
g	CA-NX-NX	Trans	115.088	585.760	NA-CN-NC

	Dihedral type	**Residue**	**Dihedral angle (degrees)**	**Force constant (kJ mol^{-1} rad^{-2})**	**Adapted from**
	CA-CA-CA-NX	All	180.0 (improper)	4.60240	CA-CA-CA-NT
	CA-NX-NX-CA	Cis	186.5 (proper)	6.27600†	X-CA-NA-X
	CA-NX-NX-CA	Trans	180.1 (proper)	6.27600†	X-CA-NA-X
	CA-CA-NX-NX	Cis	227.4 (proper)	6.27600	X-CA-NA-X
	CA-CA-NX-NX	Trans	180.1 (proper)	6.27600	X-CA-NA-X

†*Set to 1000 kJ mol^{-1} rad^{-2} for production runs*

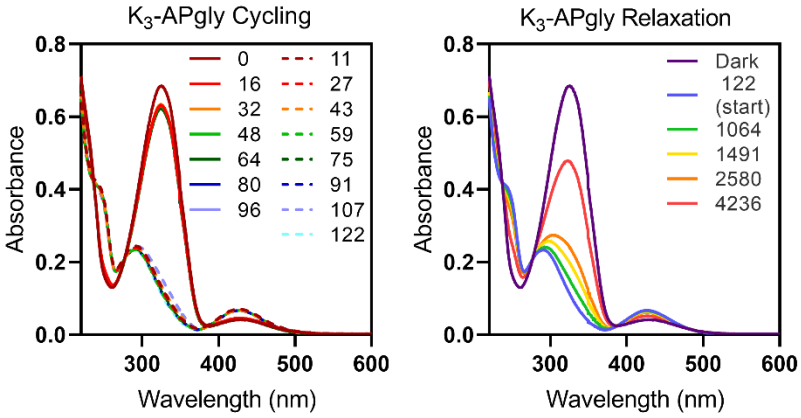

Figure S5.5: UV-Vis spectra of peptide K_3-APgly cycling between different photostationary states (left) and relaxing from the 340 nm PSS (right), which were used to prepare **Figure 5.5**. Spectra after illumination with 340 nm light are indicated with dotted lines (left). Graphs are numbered by time after start of the experiment. Measurements were performed at 20 °C in PBS with [peptide] = 50 µM.

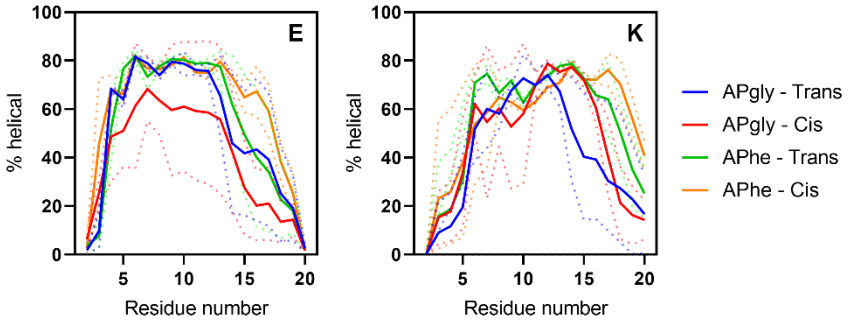

Figure S5.6: Percentage of amino acids classified as helical (based on GROMACS' default criteria for psi/phi dihedral angles and H-bond distances) over 500 ns of simulation time, for all amino acids in peptide E (left) and peptide K (right), averaged over 3 independent MD simulations. Standard deviations are plotted as dotted lines.

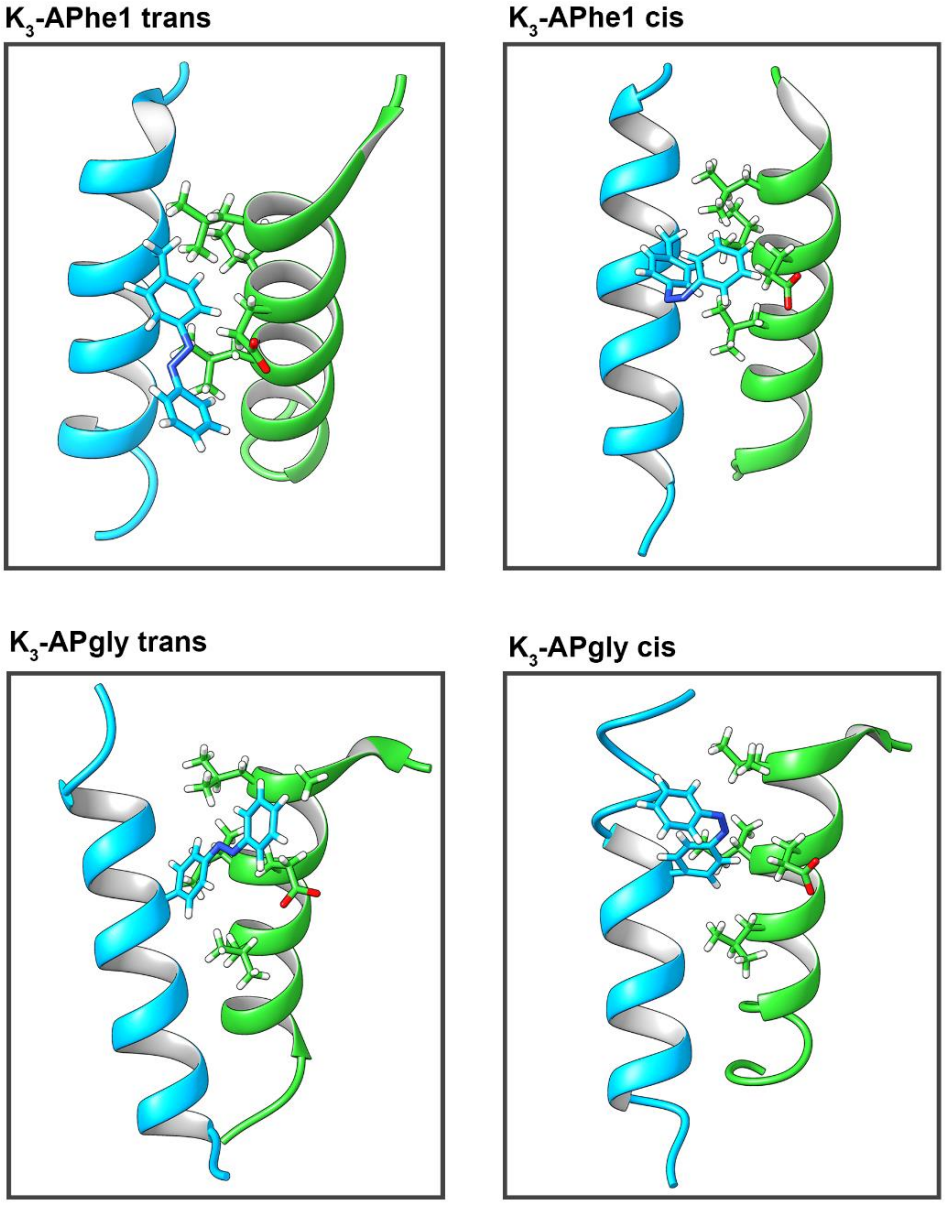

Figure S5.7: Snapshots from MD simulations of the coiled coil between peptide K_3 (blue) and E_3 (green), with peptide K_3 containing the photoswitchable amino acid **APhe1** or **APgly** at position 9 in the peptide sequence, in the *trans* or *cis* conformation. Peptides backbones are shown as a cartoon, with the photoswitch and all amino acid side chains of peptide E_3 within 5 Å displayed as sticks.

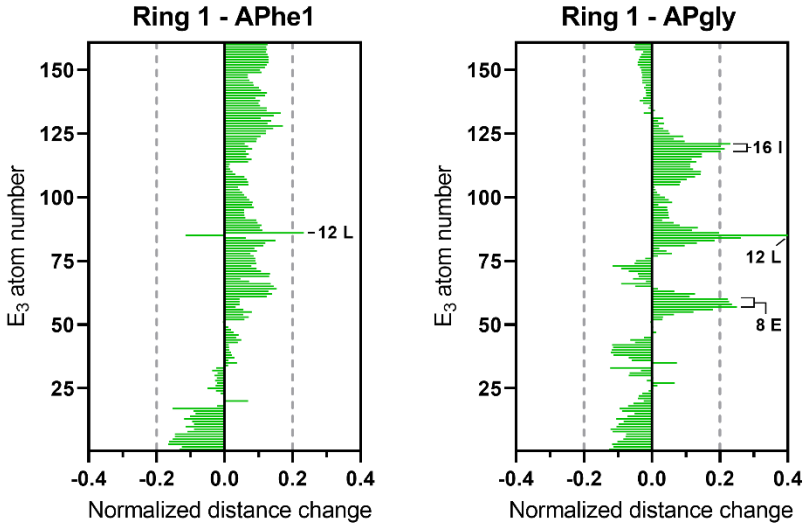

Figure S5.8: Normalized change in distance upon photoisomerization between the non-hydrogen atoms in peptide E_3 and the azobenzene ring 1 (closest to the peptide backbone). Change in distance upon *trans* to *cis* isomerization of the azobenzene is normalized to the *trans* conformation, with positive values indicating more distance in the *cis* conformation. Distances are averaged over 3 simulations of 500 ns. Dotted lines indicate an arbitrary cut-off for significance of 0.2.

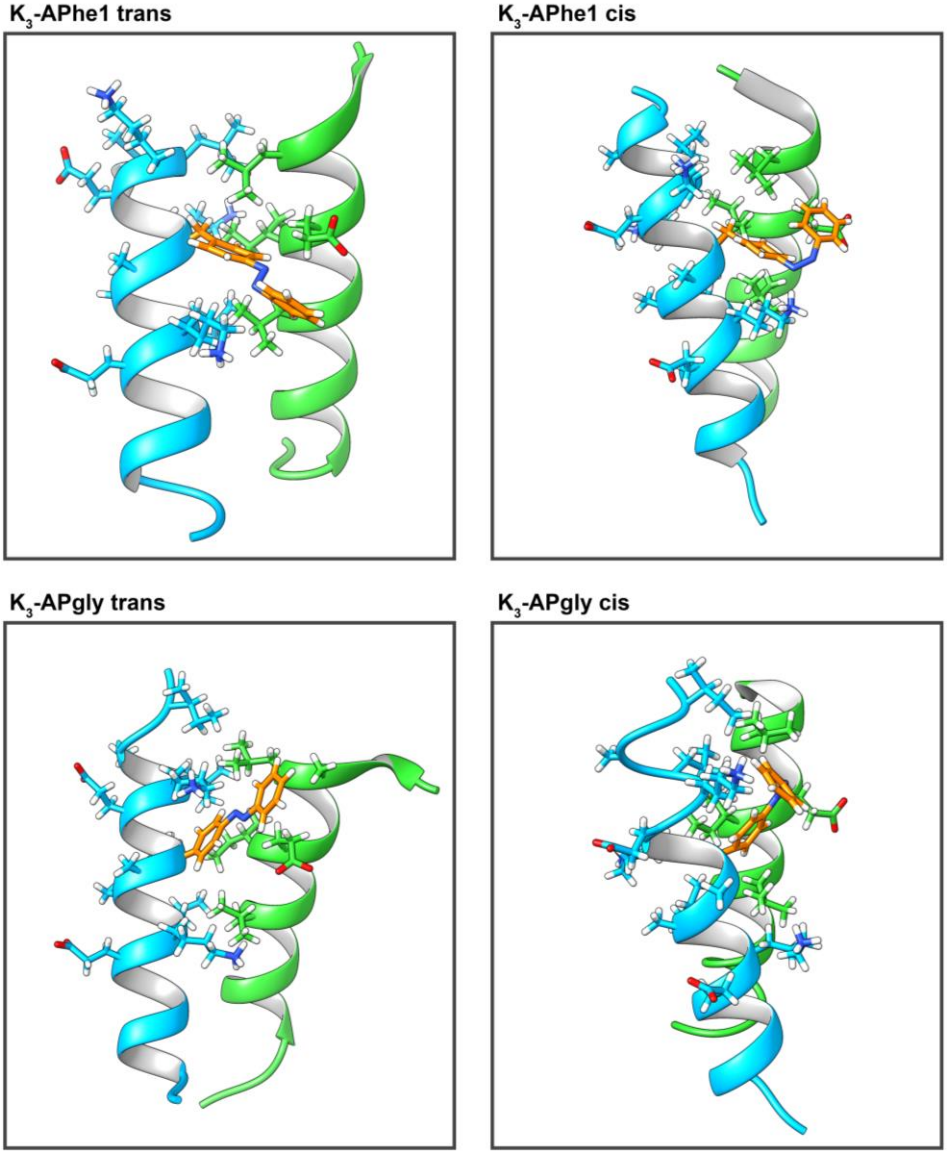

Figure S5.9: Snapshots from MD simulations of the coiled coil between E_3 (green) and K_3 (blue) containing **APhe1** or **APgly** at position 9 in the peptide sequence, in either the cis or *trans* conformation. Photoswitchable amino acids in peptide K_3 have been coloured orange for clarity. Peptides backbones are shown as a cartoon, with the photoswitch and all amino acid side chains within 5 Å displayed as sticks.

LC-MS of purified peptides

Table S5.4: Overview of the calculated masses of all peptides used in this project, and the masses found by LCMS.

Peptide name	Calculated mass (Da)	Measured mass (Da)
E_3GY	$[M + 2H^+]^{2+}$ 1272.69	1271.24
	$[M + H^+]^+$ 2544.39	2545.88
K_3-P9-APhe1	$[M + 2H^+]^{2+}$ 1230.24	1228.81
K_3-P9-APhe2	$[M + 2H^+]^{2+}$ 1252.24	1250.85
K_3-P9-APgly	$[M + 2H^+]^{2+}$ 1223.23	1222.23